

Structural and hydraulic response of emerged low-crested cube-armoured breakwaters

Yuksel, Yalcin; Cevik, Esin; Sahin, Cihan; van Gent, Marcel R.A.; Gumus, Serhat; Issever, Duygu; Inal, Umutcan; Ogur, Mehmet Utku

DOI

[10.1016/j.apor.2025.104488](https://doi.org/10.1016/j.apor.2025.104488)

Publication date

2025

Document Version

Final published version

Published in

Applied Ocean Research

Citation (APA)

Yuksel, Y., Cevik, E., Sahin, C., van Gent, M. R. A., Gumus, S., Issever, D., Inal, U., & Ogur, M. U. (2025). Structural and hydraulic response of emerged low-crested cube-armoured breakwaters. *Applied Ocean Research*, 156, Article 104488. <https://doi.org/10.1016/j.apor.2025.104488>

Important note

To cite this publication, please use the final published version (if applicable). Please check the document version above.

Copyright

Other than for strictly personal use, it is not permitted to download, forward or distribute the text or part of it, without the consent of the author(s) and/or copyright holder(s), unless the work is under an open content license such as Creative Commons.

Takedown policy

Please contact us and provide details if you believe this document breaches copyrights. We will remove access to the work immediately and investigate your claim.



Research paper

Structural and hydraulic response of emerged low-crested cube-armoured breakwaters

Yalcin Yuksel^{a,*}, Esin Cevik^a, Cihan Sahin^a, Marcel R.A. van Gent^b, Serhat Gumus^a, Duygu Issever^a, Umutcan Inal^a, Mehmet Utku Ogur^a

^a Yildiz Technical University, Department of Civil Engineering, Esenler 34210, Istanbul, Turkey

^b TU Delft and Department Coastal Structures & Waves, Deltares, Delft, The Netherlands



ARTICLE INFO

Keywords:

Low-crested breakwater
Cube armour
Climate change
Wave transmission
Stability
Packing density
Crest width
Physical model tests

ABSTRACT

In this study, the structural and hydraulic behavior of statically stable emerged low-crested cube-armoured breakwaters were investigated by performing physical model tests. This research considered cube armour layers with irregular placement in a double layer and cube armour layers with a regular placement in a single layer. For the single layer placement, two different packing densities were tested ($\psi=0.59$ and 0.67) because optimizing the packing density is relevant for the ease of construction, lowering the environmental impact and for the costs of cube armour layers. Low-crested breakwaters with both regular and irregular placements were considered with three different crest widths. The armour stability, wave transmission and wave reflection of emerged type low-crested breakwaters using concrete blocks were investigated experimentally under irregular wave conditions. The results show that for cube-armoured low-crested breakwaters with irregular placement, the cube dimensions can be significantly reduced compared to conventional rubble mound breakwaters with higher crests. The structural stability of low-crested breakwaters with single-layer regular placement showed different responses compared to the irregular two-layer case due to the geometric discontinuity at the intersection of the front slope and crest. Although the regularly placed single armour layer is more stable than the irregularly placed double armour layer with the same packing density ($\psi=0.59$), damage to the crest is more critical, causing instability of the structure for the single armour layer. For the single-layer regular placement with the smaller packing density ($\psi=0.59$), damage occurred on the front slope and crest, while for the higher packing density ($\psi=0.67$) relatively limited damage was observed on the crest only. For the hydraulic behavior of low-crested breakwaters with cube armour layers, the incident wave conditions, the freeboard (R_c) and crest width (B) are the most important parameters. It is evident that for low-crested breakwaters, the wave transmission increases but the reflection decreases compared to conventional breakwaters with a high crest. Based upon a re-evaluation of expressions given in literature on wave transmission and wave reflection at rubble mound low-crested breakwaters, new formulas for cube-armoured structures have been obtained. Hence, this study provides further information and guidance on applications for engineers and researchers on the structural and hydraulic response of low-crested cube-armoured breakwaters because increasing water levels, wave heights and storm frequencies due to global climate change are driving the need for more resistant coastal structures, adaptation measures and improvements in the design of low-crested breakwaters.

1. Introduction

Global climate change has motivated scientists and engineers to design and construct environmentally friendly and sustainable coastal structures. Since global climate change causes sea level rise and potentially increases the intensity and duration of storms, new studies on low-

crest breakwaters are needed. Since these structures are both environmentally friendly and more economical than conventional non-overtopped structures, they are expected to be used more frequently in the future.

Increasing environmental risk due to global climate change, erosion, coastal flooding and port investment will cause serious problems.

* Corresponding author.

E-mail addresses: yalcinyksl@gmail.com (Y. Yuksel), marcel.vangent@deltares.nl (M.R.A. van Gent).

<https://doi.org/10.1016/j.apor.2025.104488>

Received 17 August 2024; Received in revised form 6 February 2025; Accepted 23 February 2025

Available online 1 March 2025

0141-1187/© 2025 The Authors. Published by Elsevier Ltd. This is an open access article under the CC BY license (<http://creativecommons.org/licenses/by/4.0/>).

Therefore, more resilient structures such as breakwaters are needed to protect coastal areas and ports. As long as conventional rubble mound breakwaters are high enough to prevent wave overtopping, the armour on the crest and rear slope can be smaller than that on the front slope. Most structures, however, are designed to have some or even severe wave overtopping under design conditions. On the contrary, other structures are so low that even under daily wave conditions, the structures are overtopped. Breakwaters with the crest level around still water level and sometimes far below it, will always be subjected to overtopping and cause transmission of waves, these types of structures are called low-crested breakwaters (LCBs). It is obvious that when the crest level of a structure is low, wave energy can pass over the structure. This has two effects: First, the armour on the front slope can be smaller than the conventional type breakwater due to the fact that less energy is left on the front slope resulting in lower run-down forces. The second is that crest and rear slope must be armoured which can withstand the attack by overtopping waves.

Low-crested rubble mound breakwaters (LCBs) can be divided into three categories: dynamically stable reef breakwaters, statically stable low-crested emerged type structures and statically stable submerged structures (Van der Meer and Daemen, 1994). A reef-type breakwater consists of homogeneous rocks without filter and core layers. The crest of this breakwater is initially above the water level and under storm wave conditions, the crest height reshapes below the water level. Statically stable LCBs are mainly wave overtopped structures. But they are more stable due to the fact that a (large) part of the wave energy can pass over the breakwater.

LCBs have been studied for many years, and there are various studies on the stability and wave transmission of these structures in the literature. The studies on the structural response of LCBs were carried out under specified boundary conditions (Powell and Allsop, 1985; Givler and Sørensen, 1986; Ahrens 1987; 1989; Van der Meer, 1990; Vidal et al., 1992; 1995; Burger, 1995; Burcharth et al., 2006; Muttray et al., 2012). These studies mostly concentrated on structures with rock in the armour layer. Van der Meer (1990) gave an expression regarding the decrease in rock size in the armour layer for rubble mound LCBs. Some essential studies on LCBs are given in Table 1 with their validity conditions.

The hydraulic response of LCBs involves a complex interaction of

Table 1
Literature on LCBs stability.

Authors	Remarks
Powell and Allsop (1985)	Dynamically stable LCB
Givler and Sørensen (1986)	Regular waves were used. Dynamically stable submerged breakwater. $-0.20m < R_c < 0.0m$
Ahrens (1987,1989)	An expression was proposed for the equilibrium crest height. Dynamically stable LCB.
Van der Meer (1990)	Dynamically stable LCB. Statically stable low-crested emerged and submerged breakwater. $R_c = -0.10m, 0.0m, 0.125m$
Vidal et al. (1992, 1995)	The trunk and head sections were examined. Statically stable low-crested emerged and submerged breakwater. $R_c = -0.05m$ and $0.06m$
Burger (1995)	Van der Meer (1988) and Vidal et al. (1992, 1995) results were reanalyzed. The influence of the shape and gradation of rock on stability was investigated.
Burcharth et al. (2006)	The trunk and head sections have been examined. Statically stable low-crested emerged and submerged breakwater. $-0.10m < R_c < 0.05m, B = 3D_{n50}, 8D_{n50}$ $R_c = -0.10 < R_c < 0.05, S_{op} = 0.02 - 0.035$ Wave approach angle = $(-30^\circ), (20^\circ)$
Muttray et al. (2012)	The Xbloc was used. The front slope, rear slope and crest were examined separately. $\frac{R_c}{H_s} = 0, 0.4, 0.8, B = 3D_{n50} \text{ and } 9D_{n50}, S_{op} = 0.02 - 0.04.$ Statically stable low-crested emerged and submerged breakwater.

wave transmission, reflection and energy dissipation. Optimizing these structures requires careful consideration of design parameters, environmental impacts and the dynamic marine environment. In this type of breakwaters, wave transmission occurs with wave overtopping and wave propagation from the permeable structure to the rear side. The amount of wave overtopping is affected by the crest freeboard and crest width.

LCBs reflect some of the incident wave energy seaward. The reflection coefficient depends on the geometry of the structure, surface roughness and incident wave conditions. LCBs typically reflect less energy than high (non-overtopped) crested breakwaters. The permeable nature and armour layer selection of LCBs, such as the use of rubble mound structures, also contribute to energy dissipation through friction and turbulence. This reduces energy transmission to the rear slope of the structure. There are many studies on the hydraulic behavior of LCBs with different geometries and permeabilities. In these studies, expressions for wave transmission, wave overshoot and wave reflection were given (Van der Meer and Pilarczyk, 1990; Daemen, 1991; Ahrens, 1987; Van der Meer and Daemen, 1994; d'Angremond et al., 1996; Seabrook and Hall, 1998; Calabrese et al, 2002; Briganti et al., 2003; Van der Meer et al., 2005; Buccino et al., 2007; Goda and Ahrens, 2008; Tomasicchio and D'Alessandro, 2013; Zhang and Li, 2014; Sindhu and Shirlal, 2015; Giantsi and Moutzouris, 2016; Kurdistani et al., 2022; Van Gent et al., 2023). Some major studies on the hydraulic responses of low-crested breakwaters are given in Table 2. In recent years, studies have been carried out for structures similar to LCBs that allow wave transmission using different structural materials, attempting to determine the hydraulic behavior of the structure under wave influence (Guo et al., 2022, 2023a, b).

Some parameter definitions used in Tables 1 and 2 are H_s =incident significant wave height at the toe of the structure (from time-domain analysis), H_{m0} =spectral incident wave height at the toe of the structure, H_t =transmitted wave height, typically H_{m0t} is the spectral transmitted wave height at the rear side of the structure, T_p =peak wave period, $T_{m-1,0}$ =spectral wave period, s_{op} =wave steepness, $s_{op} = 2\pi H_{m0} / (gT_p^2)$, $s_{m-1,0}$ =spectral wave steepness, $s_{m-1,0} = 2\pi H_{m0} / (gT_{m-1,0}^2)$, R_c =crest freeboard (positive for emerged structures, negative for submerged structures, zero at still water level), h_c =structure height (from toe to crest), B =crest width, D_{n50} =nominal diameter of armour units, d =water depth at the toe, K_t =transmission coefficient, H_{m0t}/H_{m0i} , R_c/H_{m0} =relative crest height, $B/L_{m-1,0}$ =relative crest width, ξ_{op} =breaker parameter based on peak wave period, $\xi_{op} = \tan\alpha / (s_{op})^{0.5}$, $\xi_{m-1,0}$ =breaker parameter based on spectral wave period, $\xi_{m-1,0} = \tan\alpha / (s_{m-1,0})^{0.5}$, $\tan\alpha$ =slope of structure.

In the literature, rock is mostly used in the armor layers of classical LCBs, but there is no detailed study for concrete block armor layers. As is known, conventional breakwaters with cube armor layers are designed either with two-layer irregular placement or with a single-layer regular placement (Yuksel et al., 2020 and 2022, Van Gent et al., 1999). The typical instability of conventional breakwaters which have an armour layer consisting of a single layer of cubes without wave overtopping, is sudden failure due to chain reaction risk in the armour layer stability. For this reason, the relative damage $N_0 = 0.2$ is used for the failure of the armour layer which is defined in Section 3 (visible filter layer) because once the damage starts, it progresses rapidly and due to the lack of resistance, the filter layer underneath is immediately exposed. On the other hand, some damage is allowed in the double-layer conventional breakwater with cubes, and for the relative damage $N_0 = 0.5$ can be taken as criterion (Van der Meer, 1999).

In this study, the structural stability and hydraulic responses of statically stable emerged LCBs were investigated experimentally under irregular wave conditions. A LCB can be considered as a statically stable conventional breakwater that allows (significant) wave overtopping. Unlike other studies in the literature for LCBs listed in Table 1, in this study, cube concrete blocks, which are easy to manufacture, were used in the armour layers. Different placements of the cube blocks in the

Table 2
Literature on LCBs for wave transmission.

Authors	Remarks
Van der Meer and Pilarczyk (1990)	Low-crested submerged and emerged breakwaters. $-1.13 < \frac{R_c}{H_s} < 1.2, -2.00 < \frac{R_c}{H_s} < -1.13, 1.2 < \frac{R_c}{H_s} < 2$
Daemen (1991)	Low-crested submerged and emerged breakwaters (statically stable breakwaters). $1 < H_s/D_{n50} < 6, 0.01 < s_{op} < 0.05, -2.00 < \frac{R_c}{H_{m0}} < 2$
Ahrens (1987)	Low-crested emerged breakwaters. $1.2 < \frac{R_c}{H_s} < 2$
Van der Meer and Daemen (1994)	Low-crested submerged and emerged breakwaters. $1 < H_s/D_{n50} < 6, 0.01 < s_{op} < 0.05$
d'Angremond et al. (1996)	Low-crested submerged and emerged breakwaters. Permeable and impermeable breakwaters. $s_{op} < 0.06, -2.5 < \frac{R_c}{H_s} < -2.5, \frac{H_s}{d} > 0.54$
Seabrook and Hall (1998)	Low-crested submerged breakwaters. $5 \leq \frac{B}{H_s} \leq 74.47, 0 < \frac{B(-R_c)}{LD_{n50}} < 7.08, 0 < \frac{H_s(-R_c)}{BD_{n50}} < 2.14$
Calabrese et al. (2002)	Low-crested submerged and emerged breakwaters in presence of broken waves. $-0.4 \leq \frac{R_c}{B} \leq 0.3, 1.06 \leq (B/H_{m0}) \leq 8.13,$ $0.31 \leq \frac{H_{m0}}{d} \leq 0.61; 3 \leq \xi_{op} \leq 5.2$
Briganti et al. (2003)	Low-crested submerged and emerged breakwaters. $\frac{B}{H_s} > 10, \xi_{op} < 3$
Van der Meer et al. (2005)	Low-crested submerged and emerged breakwaters. $1 \leq s_{op} \leq 3, 0^\circ \leq \beta \leq 70^\circ, 1 \leq \frac{B}{H_s} \leq 4, \frac{B}{H_s} > 12$
Buccino et al. (2007)	Low-crested submerged breakwaters. $0 \leq \frac{R_c}{H_s} \leq 2,$ $1 \leq \xi_{op} \leq 8$
Goda and Ahrens (2008)	Low-crested submerged and emerged breakwaters for rubble stone and concrete blocks.
Tomasicchio and D'Alessandro (2013)	Revised Goda and Ahren's (2008) equation
Zhang and Li (2014)	Low-crested submerged and emerged breakwaters (permeable and pile type breakwater).
Sindhu and Shirlal (2015)	Low-crested submerged breakwaters.
Giantsi and Moutzouris (2016)	Revised d'Angremond's equation.
Kurdistani et al. (2022)	Low-crested submerged breakwaters.
Van Gent et al. (2023)	Submerged and low-crested structures (impermeable, permeable and perforated structures). $-2.5 < \frac{R_c}{H_{m0}} < 0,$ $\frac{R_c}{H_{m0}} = 0.5, 0.015 < s_{m-1.0} < 0.033,$ $0.017 < \frac{B}{L_{m-1.0}} < 0.075, 0.9 < \frac{B}{H_{m0}} < 2.3$

armour layer, i.e., irregular (double layer) and regular (single layer), were considered. Single-layer cubes could be a significant alternative to other single-layer armour units (Yuksel et al., 2020, 2022; Van Gent et al., 1999) as this placement technique may become more stable than double-layer irregular placement. The strength of single layers is a combination of the strength due to weight (also valid for double layers) and the strength due to contact forces between the adjacent blocks (as for placed block revetments) with less wave attack acting on single units due to smoother surface of the entire slope. Moreover, the use of concrete armour cubes in a single layer is a feasible and cost-effective solution, especially when compared to other double-layer concrete units (such as Tetrapod and Antifer) and even some single-layer concrete units (such as Core-Loc and Accropode). Additionally, the application of concrete cube elements does not incur licensing fees, which is also considered an advantage. Besides, most of the LCBs have rock as armour layer, and the supply of quarry stone can cause unfavorable environmental impacts. However, there is no detailed research on the structural and hydraulic behavior of cube-armoured LCBs. In the present study, the structural stability, and wave transmission and reflection of

cube-armoured LCBs were studied for different placement conditions and also for different crest widths. It has been determined how much the cube dimensions can be reduced in LCBs compared to conventional breakwaters that do not allow wave overtopping. Since this type of cube armour layers can be placed with different packing densities, the effect of the packing density on the stability and hydraulic response, especially in regular placement, has also been investigated. Thus, new design concepts and expressions were put forward for the low-crest breakwater with a cube armor layer. The paper is organized as follows: Section 2 explains the experimental setup and LCBs model descriptions. In Section 3, structural and hydraulic behaviors of the LCB models are discussed, new formulas are also presented for wave transmission and wave reflection. Finally, in Section 4, the most significant conclusions from this experimental study are given and suggestions for future research are highlighted.

2. Experimental setup and methodology

The experiments were carried out in the 26 m long, 1.0 m wide and 1.0 m high wave channel located in the Hydrodynamic Research Laboratory at Yildiz Technical University. There is a wave generator with a wave absorption system in the wave channel. At the other end of the wave channel, there is a passive absorption system consisting of gravel and porous damping (Fig. 1). The statically stable low-crested emerged type breakwater (LCB) model was designed at a scale of 1/30, considering that the core would remain at least 1.0 m above the water level in prototype conditions. The water depth was 0.60 m. During the experiments, emerged statically stable LCBs with cube armour layers were studied (Fig. 2).

During the tests, the water level behind and in front of the LCB model was kept constant with the help of drainage pipes placed at the bottom, and the water level at the back of the LCB was not allowed to rise. The breakwater model was placed on a horizontal foreshore with 1:1.5 structure slopes on both sides. The tested structures consist of cube armour layers with a size of $D_n=40$ mm and a density of 24 kN/m^3 on top of a permeable core of stones with a size of $D_{n50}=19$ mm. The standard Froude scaling method for the underlayer, which is the core material, is based on a ratio between the armour block weight and the underlayer material weight, $M_{\text{armour}}/M_{50, \text{underlayer}}$. A relation based on the nominal diameter of the armour and underlayers $D_{n, \text{armour}}/D_{n50, \text{underlayer}}$ is also commonly used. Van Gent (2003) recommended a ratio between 2 and 2.5. In the present study, this ratio was considered as $D_{n, \text{armour}}/D_{n50, \text{underlayer}} = 40/19 = 2.1$ for both models.

The packing density of double-layer irregular placement was 0.59. However, in single-layer regular placement methods, two different packing densities were used: 0.59 and 0.67 (Fig. 3). Before placing the cubes for both placement methods, the number of cubes for each row was calculated by taking into account the model width. The cubes at each side boundary of the wave flume were not taken into account in the stability calculations due to potential wall effects. For the irregular placement, the blocks were placed by letting them fall free from a height of half a nominal diameter above to ensure the irregularity of the placement (Fig. 3a). However, blocks were placed one by one to each calculated location on the slope for regular placement; they were placed staggered over the slope as seen in Fig. 3b. For both placement methods, the units were placed in colored bands to improve the visualization of the displacement and so to measure the damage easily.

The model is such that it allows wave overtopping and wave propagation through the armour layer and core of the model. Reflection analysis based on the Mansard and Funke (1980) method was performed by placing four wave probes in the front of the LCB as shown in Fig. 1, to obtain the incident waves. Behind the breakwater model, a wave probe was placed to measure the transmitted waves, and a point gauge was placed to control the water level. A passive absorption slope of 1/5 at the back end of the flume was placed to prevent the reflection of the

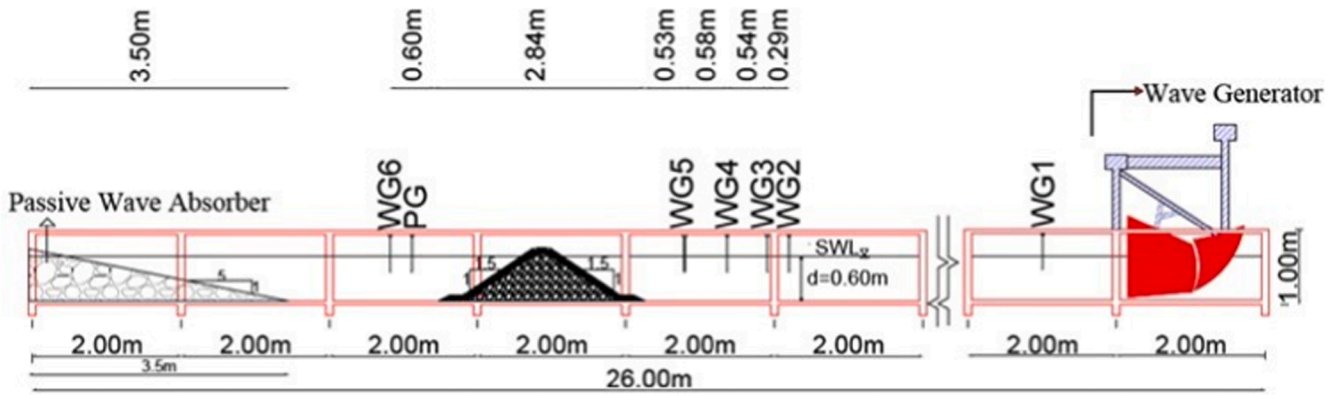


Fig. 1. Longitudinal cross-section of the wave flume.

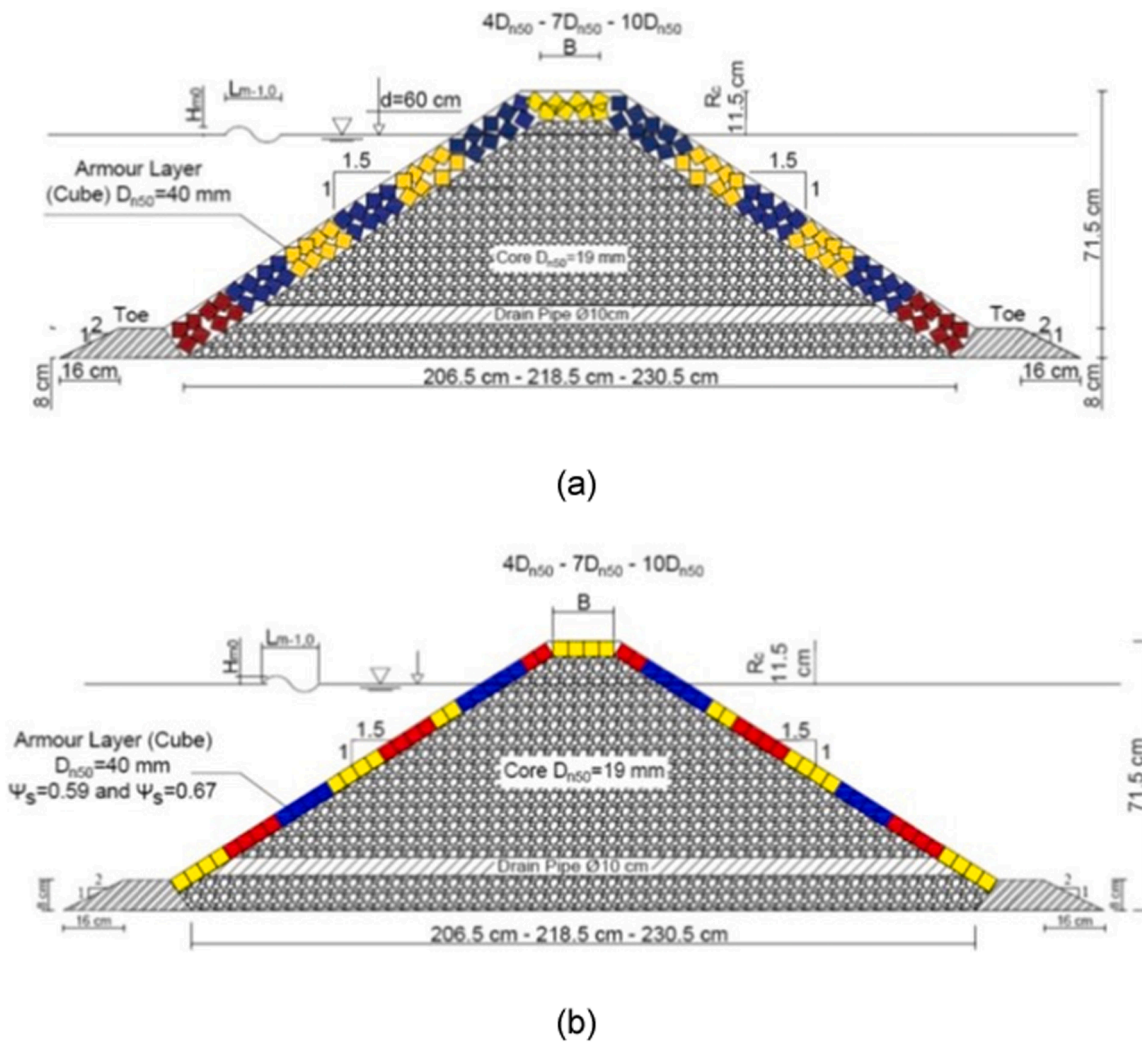


Fig. 2. LCB models, (a) Double-layer irregular placement and (b) Single-layer regular placement.

transmitted waves. Although the wave generator has an active wave absorption system, waves were also measured by placing four probes in front of the passive absorption system (gravel and porous surface) in the absence of a structure (LCB). It was determined that the incident wave conditions of the set-up with and without the rubble mound structure were comparable, and the experimental results were evaluated with the help of the incident wave conditions at the toe of the structure without the structure in place. In this study, the spectral significant wave height

H_{m0} (in this study: $H_{m0}=4(m_0)^{0.5}$) and spectral wave period $T_{m-1.0}$ ($T_{m-1.0}=m_{-1}/m_0$) were obtained from the measured wave energy spectrum.

The Reynolds numbers were also checked to avoid scale effects. The viscous scale effect is ignored when the Reynolds number is higher than 2×10^3 (Hughes, 1993; Andersen and Burcharth, 2010; Wolters et al., 2010). The Reynolds number was calculated by $Re = UD_n/\nu$ where D_n is the characteristic dimension of the armour material (nominal diameter)

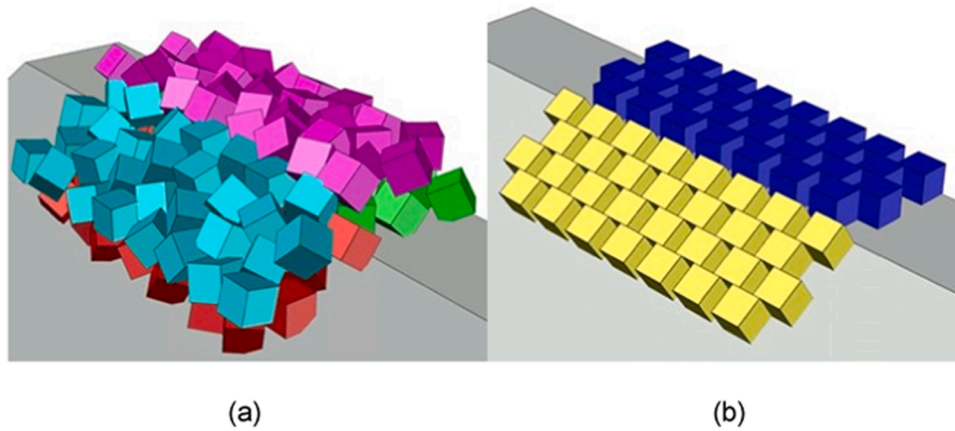


Fig. 3. Irregular (a) and regular (b) placement styles.

and ν is the kinematic viscosity, which for water at 10° is $1.33 \times 10^{-6} \text{ m}^2/\text{s}$ where U is the seepage velocity $U = (P.H_s.L_m)/(2.d.T_m)$, where P is the porosity of the core material, H_s is the significant wave height at the toe, L_m is the mean wavelength of the waves, and T_m is the mean wave period at the toe. The Reynolds number was 5×10^3 for the typical values used in this study, i.e., $P=0.49$, $H_s=0.14 \text{ m}$, $T_m=1.16 \text{ s}$, $d=0.60 \text{ m}$, $D_{n50}=0.019 \text{ m}$, which indicates that experiments are not influenced by scale effects. However, in a small-scale physical model, the friction forces between units may not be equal to those in the prototype because the cube unit surface can be relatively rougher in the model than for the large-scale units. As painting the unit provides a somewhat smoother surface, all units were painted with different colors (Yuksel et al., 2022).

The toe stability of the structure was out of the scope of this research. The toe was fixed with a steel frame in order to avoid the toe stability problem for all cases, hence it did not affect the stability of the slope (Yuksel et al., 2022). The width and the thickness of the toe were $4D_n=16 \text{ cm}$ and $2D_n=8 \text{ cm}$, respectively.

A total of 15 irregular wave conditions with a JONSWAP spectrum ($\gamma = 3.3$) in deep water were selected for all stability tests and 10 additional waves for transmission tests. Wave conditions were measured by wave probes at six different locations. One of them is placed in front of the wave generator. One of them is placed behind the model to measure transmitted waves. Four other probes were placed in front of the model at known intervals to separate the incident and reflected waves (Fig. 1).

For each test, the significant wave height in front of the toe was gradually increased to identify the wave height that caused cumulative damage. The design wave height was determined as $H_s=0.20 \text{ m}$ based on the cubes and physical scale (1/30). On the other hand, the progression of the damage was determined by producing waves beyond the design wave. The design wave was increased only by around 10% due to the limitations of larger waves according to the selected model dimensions, wave generator capacity, and water depth at the toe of the structure. Stability tests were repeated to check consistency.

The damage was repaired after each experimental condition run, but not after each test run (a total of 15 tests for each experimental condition). Both placement methods were tested for a wave steepness $s_p = 2\pi H_s/gT_p^2 = 0.033$.

Each test run consisted of approximately 1000 waves. Damage was detected using a visualization technique by taking camera recordings and digital photos before and after each test run from fixed positions perpendicular to the front and rear slopes using two cameras. Damage was determined by counting armour units moved and displaced relative to the width (along the longitudinal axis of the breakwater) of the nominal diameter (D_n) from digital photographs. As indicated before, in order to avoid possible side wall effects that could affect the results, $1D_n$ widths from both sides of the wall were not considered in the damage evaluation (Frens, 2007; Van Gent, 2013; Yuksel et al., 2020, 2022).

Table 3

Ranges of the parameters for the experimental data set.

Parameter	Symbol	Value
Slope angle	$\cot\alpha$	1.5
Relative density for cubes and underlayers	Δ	1.4 and 1.65
Cube size (m)	D_n	0.040
Grading underlayer material (core)	D_{n85}/D_{n15}	1.38
Crest width (m)	B	0.16, 0.28, 0.40
Crest freeboard (m)	R_c	0.115
Structure height (m)	h_c	0.715
Water depth at toe (m)	d	0.60
Wave steepness, ($s_{m-1,0} = 2\pi H_s/gT_{m-1,0}^2$ here $H_s=H_{m0}$)	$s_{m-1,0}$	0.020 - 0.050
Wave steepness ($s_p = 2\pi H_s/gT_p^2$ here $H_s=H_{m0}$)	s_p	0.020 - 0.040
Relative water depth at toe (here $H_s=H_{m0}$)	d/H_s	≥ 3.0
Wave height ratio (here $H_s=H_{m0}$)	$H_{2\%}/H_s$	1.4
Number of waves	N	1000
Stability number (here $H_s=H_{m0}$)	$N_s=H_s/\Delta D_n$	0.36 - 3.89

Table 3 provides an overview of the most important parameters for all placements.

Experiments were carried out under the following model conditions:

1-Three different crest widths of the structure were $B=4D_n, 7D_n$ and $10D_n$, representing the narrow, transitional and wide crest conditions.

1-Double-layer irregular placement of cube blocks on the armour layer of the model (DLC case) with packing density (ψ) of 0.59.

2-Single-layer regular placement of cube blocks (SLC case) with packing densities of (ψ) 0.59 and 0.67.

The main characteristics are:

1- Emerged, statically stable LCB model.

2- The crest elevation was kept constant for both irregular double-layer (DLC) and single-layer regular (SLC) placement cases.

As mentioned before, when determining the crest freeboard, the scale ratio was considered as 1/30, assuming that the crest of core remained at least 1.0 m above the still water level in situ. The reason why the crest of the core is considered above the still water level is for the ease of construction point of view in situ. For both cases (DLC and SLC cases), the crest level of the core was adjusted in order to keep the crest freeboard (0.115 m) the same.

3-Rigid toe.

4-Horizontal foreshore slope.

3. Results and discussion

3.1. Structural responses

In this study, damage is taken into account separately as movement

(M) and displacement (D) of the cubes. Damage is defined for displaced units as follows (Frens, 2007; Yuksel et al., 2020, 2022):

- No damage: No units are displaced.
- Initial damage: A few units are displaced.
- Failure: The underlayer is exposed to direct wave attack.

Damage was calculated and evaluated as follows:

1-Displacement ratio was calculated using the equation given below:

$$\text{Displacement Ratio (D}_1\text{)} = \frac{\text{Number of displaced units}}{\text{Total number of units within reference area}} \quad (\%) \quad (1)$$

$$N_0 = \frac{\text{Number of displaced units of one nominal diameter } D_n \text{ in reference area}}{L/D_n} \quad (2)$$

The displacement of units is defined as the movement of a block more than one D_n length (Van der Meer, 1988) from its original position. The displacement ratio was classified as

- D_1 represents the displacements between $1.0D_n$ and $2.0D_n$,
- D_2 is above $2.0D_n$
- D_T is above $1.0D_n$. Hence, D_T considers all (total) displaced cubes in the reference area (Frens, 2007; Yuksel et al., 2020, 2022).

Movement is considered as an action of mobility which can be defined as an amount of displacement less than $1.0D_n$.

Movement may occur before displacement, and the units may lose their support from the adjacent units. According to Eq. (1), three different categories of movement are defined in relation to the nominal diameter:

- M_1 is less than $0.5D_n$
- M_2 is between 0.5 and $1.0D_n$
- M_T is less than $1.0D_n$ (total movement).

Damage defined by movement is especially important for cube blocks, which maintain their stability by resting on and friction with each other. Moving blocks affect the stability of neighboring blocks which mostly result in displacement. Additionally, moving blocks can

hit each other and cause them to break. Therefore, the damage percentage of moving blocks is an important indicator defining structural behavior.

2- Relative damage number is the other damage definition. Damage in concrete cube blocks is defined by the actual number of displaced units (N_0) relative to a nominal diameter (D_n) width (along the longitudinal axis of the breakwater). In this study, relative damage was found by counting displaced cubes within a nominal diameter in the reference area from camera recordings.

where L is the width of the model structure excluding one nominal diameter from each side wall and D_n is the nominal diameter of the cube.

A reference area is defined to determine the damage. The reference area was defined as the area between two levels of $SWL \pm H_{m0}$, which corresponds to $SWL \pm 5D_n$ for the selected design wave height of $H_{m0} = 0.20$ m and nominal cube diameter of 4 cm (Yuksel et al., 2020, 2022). The design wave height was determined by considering the conditions of the wave flume and the physical model conditions for stability and wave transmission of the modeled low-crest breakwater. In this study, the reference area for the breakwater model was kept constant at $10D_n$ below the crest for both the front and rear slopes.

(i) Double-Layer Irregular Placement

The experiments were carried out with a set of 15 consecutive increasing wave heights, while each condition lasted 1000 waves. No repair was carried out between these 15 conditions, so the cumulative damage was determined. Although the design wave height was chosen as 20 cm in the experiment, waves beyond the design wave height were also tested. The incident wave height varied between 0.02m and 0.22m, and the spectral wave period varied between 0.83s and 2.02s. The wave conditions applied at each crest width were kept the same. For the tests with cubes in a double layer, the cubes were placed irregularly. The reflection coefficients were determined by analyzing the signals of the four probes placed in front of the model. The average reflection of all wave conditions was 0.42. The incident and reflected waves at the model toe were separated with the reflection analysis and the stability was evaluated using the incident waves. The experiments were repeated at least 3 times to check their repeatability.

For each crest width (B), moving and displaced blocks in the reference area of the front and rear slopes were determined. The movement ratio of cubes is plotted against the stability number for three different crest widths and is given in Fig. 4. It is seen that as the crest width increases, the number of moving blocks on the front slope decreases relatively. While the movement ratio of blocks for $B = 4D_n$ and $7D_n$ increased to around 40%, this rate remained around 24% for $B = 10D_n$. Moreover, mobility began to decline for waves higher than the design wave.

After the first three waves, overtopping begins over the crest. The amount of wave overtopping decreases as the crest width increases. For

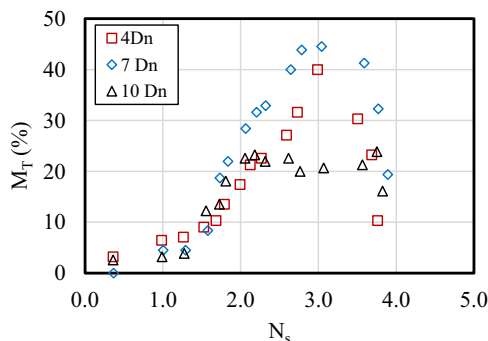


Fig. 4. Movement ratio M_T (%) versus stability number (N_s) on the front slope.

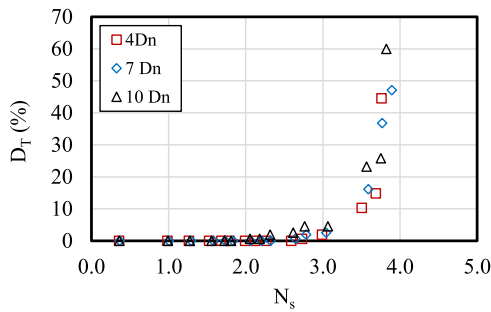


Fig. 5. Displacement ratio D_T (%) versus stability number (N_s) on the front slope.

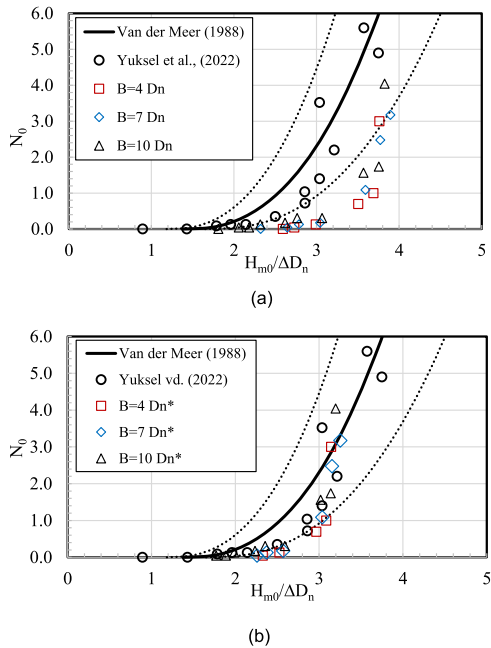


Fig. 6. Relative damage versus stability number. The dashed lines indicate the boundaries of the 90% confidence interval, (a) Comparison of relative damage on front slope (double layer irregularly placed cubes) with conventional cube armoured breakwater and (b) Relative damage after taking into account the reduction factor on the front slope for LCBs.

the widest crest, $10D_n$, the movement begins to decrease earlier and is replaced by displacement. On the other hand, it can be thought that as the mobility continued for a while for $4D_n$ and $7D_n$, the cubes started to lean on each other more, causing the stability to increase in the front slope. However, it is not desirable that cubes move too much to reduce the risk of breakage of units. Especially when the movement ratio exceeds 30%, even if the decreasing amount of movement corresponds to higher wave heights, it is not suitable for structure stability (Yuksel et al., 2020). Therefore, displacement started later in $4D_n$ and $7D_n$ crest widths than in $10D_n$, and structure stability shows almost a similar trend for all three crest widths. In other words, under the wave condition $H_{m0} = 0.13$ m, the initial instability of the structure starts for $B=4$ and $7D_n$. However, initial displacement starts at $H_{m0}=0.12$ m for $B=10D_n$ (Fig. 5).

In Fig. 5, displacement ratios (D_T) at the front slope are plotted against the stability number for all three crest widths. When this figure is examined, displacement starts earlier for the crest width of $10D_n$ and displacement started somewhat later for the $4D_n$ crest width. Nevertheless, the damage progression is very similar for all three crest widths.

In Fig. 6a, the relative damage at the front slope is plotted against the stability number. When this figure is examined, the initial damage ($N_0 > 0$) begins at $N_s=2.06$ for $10D_n$, $N_s=2.65$ for $7D_n$ and $N_s=2.73$ for

$4D_n$. However, damage evolution occurred with a similar sudden increase. Fig. 6a shows that the damage development is similar and the crest width does not have a significant effect on the development of instability, which is comparable with test results from literature (Burcharth et al., 2006). The evolution of the relative damage was compared to the breakwater with a conventional cube protection layer. In Fig. 6a, the expression by Van der Meer (1988) and data from Yuksel et al. (2022) were plotted for the same wave conditions. As can be seen from Fig. 6a, the damage at the front slope of the LCB is smaller compared to the conventional breakwater due to the occurrence of wave overtopping. However, as can be seen from the figure, the damage evolutions of these breakwater models are steeper than for the conventional breakwater. This is due to the fact that wave steepness has less effect on the stability of LCBs than on the stability of conventional breakwaters (Burcharth et al., 2006).

Failure of a double layer of cubes with irregular placement ($N_0 = 0.5$) in the front slope was reached at $N_s = 3.3, 3.2$ and 3.1 for $B = 4D_n, 7D_n$ and $10D_n$, respectively. Thus, within the limits of the experimental study, as the crest width increases, failure occurs at slightly smaller stability numbers, this result also agrees with results by Burcharth et al. (2006). Fig. 6a also shows that failure of the front slope of LCBs is reached at higher stability numbers than for conventional breakwaters.

Van der Meer (1988) indicated that the stability expression of conventional rubble mound breakwaters can be used for the stability of LCBs and that the nominal diameter, in this case, can be reduced by using a reduction expression. In this study, the reduction expression for the LCB with double-layer cubes was modified and given in expression 3.

Reduction factor equation for D_n

$$D_n^* = \frac{1}{1.25 - 1.5R_p^*} \quad (3)$$

where

$$R_p^* = \frac{R_c}{H_{m0}} \sqrt{\frac{S_{op}}{2\pi}} \quad (4)$$

$$0 < R_p^* < 0.30$$

R_c (m) refers to the crest freeboard, H_{m0} (m) is spectral wave height and S_{op} (-) is peak wave steepness. If the reduction expression (3) is applied to the present study, it can be seen in Fig. 6b that the results are compatible with the equation by Van der Meer (1988) for the conventional double-layer cube armoured breakwaters for the front slope. Fig. 6b shows that after introducing a reduction factor, the data is distributed within the 90% confidence band. In this case, the dimensions of the cube can be reduced by approximately 25% for a low-crested structure compared to the cubes applied in the conventional breakwater for the same wave conditions.

In order to investigate the effect of the relative freeboard on the stability of the front slope, the relative damage versus the relative freeboard is plotted in Fig. 7. It is seen that the relative damage increases as the relative freeboard decreases for a constant structure height in the

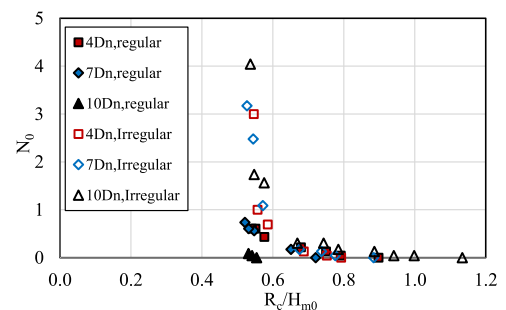


Fig. 7. Variation of relative damage with relative freeboard for front slope.

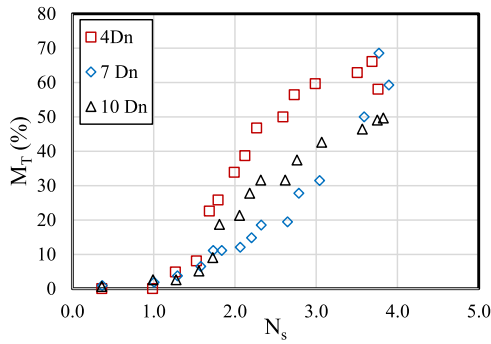


Fig. 8. Movement ratio M_T (%) versus stability number (N_s) in crest.

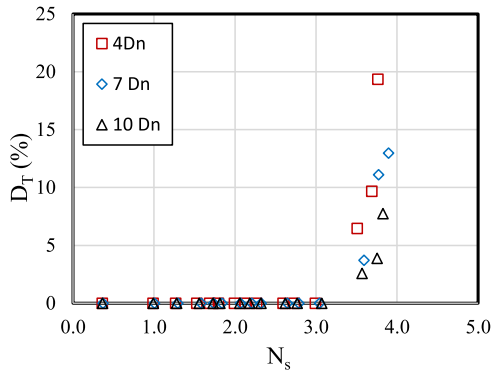


Fig. 9. Displacement ratio D_T (%) versus stability number (N_s) in crest.

limited conditions of the presented experiments. Damage suddenly increases for smaller freeboards for $R_c/H_{m0} < 0.6$ due to the increasing wave height in a constant freeboard. The stability of the low-crested cube-armoured breakwaters is significantly reduced under large wave energy conditions. It is also shown that the damage progression does not apparently change with the crest width after the limit value of 0.6. When the relative freeboard is less than 0.6, the wave conditions reach beyond the design wave height considered in this study ($H_{m0}=0.2\text{m}$), and therefore, the LCB reaches failure ($N_0 \geq 0.2$) in this case. Thus, the effect of relative freeboard no longer exists.

It is known that for the LCBs, the stability of the crest and rear slope is affected by wave overtopping, so the stability of the crest and rear slope were also studied. In Figs. 8 and 9, the movement and displacement rates on the crest are shown by plotting the damage rate (%) against the stability number.

Movements and displacements of the cubes begin primarily in the first row of the crest in contact with the front slope. It has been observed that moving and displaced blocks are pushed backwards as the wave

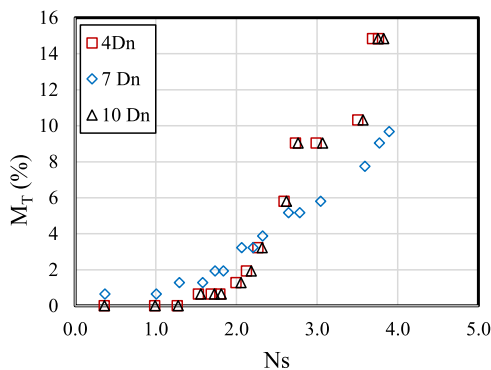


Fig. 10. Movement ratio M_T (%) versus stability number (N_s) in rear slope.

Table 4

K_{DH} Hudson stability coefficients for the front slope.

Authors	Wave conditions	Slope	Crest width (B)	K_{DH}	Wave overtopping
Van der Meer (1988)	Non-Breaking / Breaking	1/1.5	4D _n	3.27–2.25	No
Rock Manual (2007)	Non-Breaking/ Breaking	1/1.5 to 1/3.0	4D _n	7.5–6.5	No
Yuksel et al. (2022)	Non-Breaking	1/1.5	4D _n	3.80	No
Presented study	Non-Breaking	1/1.5	4D _n	13.60	Yes
Presented study	Non-Breaking	1/1.5	7D _n	12.41	Yes
Presented study	Non-Breaking	1/1.5	10D _n	5.83	Yes

height increases. When the wave height increases, the mobility in the back rows on the crest increases. The mobility rate on the crest exceeds 30% at $N_s=2.00$ for 4D_n crest width, $N_s=2.32$ for 7D_n and $N_s=2.6$ for 10D_n, as in the front slope. As the crest width increases, the mobility rate in the crest becomes slightly less.

The experiments show that the initial displacement on the crest remains almost similar as the crest width increases. The initial damage ($N_0 > 0$) is determined as $N_s = 3.51, 3.59, 3.57$ for the 4D_n, 7D_n, 10D_n, respectively for the crest. Moreover, it has been observed that the initial damage on the crest started later than on the front slope, which is due to the blocks trying to shift being pushed backwards and leaning on each other.

Movement and displacement rates in the back slope are shown in Fig. 10. M_1 type movement ($< 0.5D_n$) was found only in the back slope, and mobility never reached very large values ($< 30\%$). No displacement was observed in the rear slope.

In Table 4, K_{DH} Hudson stability coefficients of previous studies on the stability of conventional breakwaters are given together with this study. Compared to previous studies, the stability coefficients (K_{DH}) found in this study for the front slopes, as given in Table 4, are larger in LCBs that allow wave overtopping than in conventional breakwaters. However, from the observations made under the specified experimental conditions considered in this study, the probability of wave overtopping was determined to be 80%. K_{DH} decreases and becomes closer to the value of conventional breakwaters as the crest width increases because the transmission resulting from wave overtopping decreases as the crest width increases. As a result, the stability coefficient decreases as the wave transmission decreases.

(ii) Single Layer Regular Placement

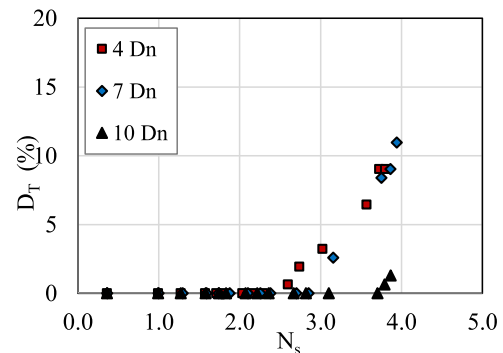


Fig. 11. Displacement rate for single layer regular placement ($\psi=0.59$) in the seaward slope.

The wave conditions in the tests of single-layer regularly placed cube models are the same as those of the double-layer irregularly placed cube models. The average reflection coefficient of the single-layer regularly placed model was obtained to be 0.45. Two different packing densities were studied for this placement case, which are 0.59 and 0.67. Crest freeboard and crest widths are kept the same as double layer irregularly placed case (Fig. 2).

The movement ratio (%) of cubes with respect to the stability number for three different crest widths of these cases were observed to have almost similar trends in both packing densities with double-layer irregularly placed models. As the crest width increased, mobility increased in this case.

In single-layer placement, the situation before the damage begins ($N_0 = 0$) is called the start of damage in the literature. On the other hand, the situation where relative damage first begins for irregular placement is defined as initial damage ($N_0 > 0$). When the variations of the displacement (D_T) ratio with the stability number for two different packing densities were examined, it has been determined that displacement occurred only if the packing density was 0.59 (Fig. 11) both on the front slope and crest. Whereas there was no displacement on the front slope, damage was slightly observed on the crest for the packing density of 0.67. The initial displacements ($N_0 > 0$) on the seaward slope are determined at stability numbers of 2.6, 3.2 and 3.8 for the crest widths of $4D_n$, $7D_n$, $10D_n$, respectively.

The damage progress with stability number is shown with 90% confidence limits using the expression given by Van der Meer (1988) for conventional breakwater with two-layer irregularly placed cube blocks in Fig. 12a and 12b. The stability numbers given in Van Gent (1999) for conventional single-layer regularly placed cube breakwater (packing density greater than 0.6) are also shown in Fig. 12, which are 3 at the start of damage (for $N_0=0$) and 3.75 at failure (for $N_0=0.2$). The damage curves of the seaward slope of all crest width models of the 0.59 packing density of the present study are shown in Fig. 12a together with the literature mentioned above. Since no damage was observed on the front slope at 0.67 packing density, it was not included in Fig. 12a.

It is clearly seen from these figures that the conventional breakwater with single-layer cube is more stable than the breakwater with double-layer irregularly placed cube blocks. However, in this study, unlike

the literature, the single-layer cube blocks for the LCB were studied at two different packing densities (0.59 and 0.67). The start of damage (for $N_0=0$) of the seaward slope is determined at stability numbers of 2.2, 2.9 and 3.7 for the crest widths of $4D_n$, $7D_n$, $10D_n$, respectively for the packing density of 0.59. These results show that the start of damage occurs before the stability number of 3 which is obtained for conventional single-layer cube-armoured breakwaters with higher packing density ($\psi > 0.6$). Only for the model with the widest crest, the start of damage occurs at the stability number of 3.7 which is higher than 3. Moreover, failure ($N_{0d}=0.2$) occurred at $4D_n$ and $7D_n$ crest width models at 3.0 and 3.2 stability numbers which are less than 3.75, i.e., the given value in the literature for the seaward slope of conventional single-layer cube-armoured breakwater, but at $10D_n$ crest width model failure was not observed within the limits of this study. These results show the effect of crest width and the packing density of single-layered breakwater on stability.

As defined in Section 2, during the stability studies of breakwaters, the active region (reference area) where the wave is effective on the seaward slope is determined and the damage in the active region is considered. In LCBs with single-layer cube armour units, the crest of the structure is always exposed to waves like active region in the front slope since the structure has a low crest, and therefore the crest can be assumed to be a part of the reference area. The geometric discontinuity at the intersection of the front slope and the crest greatly affects the stability of single-layer regular placement compared to the double-layer irregular case (Yuksel et al., 2020, 2022). However, no damage occurred on the back slope within the limits of this study, hence the front slope and crest were evaluated together and called as “the total section” for each crest width. By taking into account the above approach, the relative damage progress in the total section is presented in Fig. 12b. According to these results, at the LCB with the narrowest crest ($4D_n$), the start of damage on the front slope occurred for $N_s=2.2$. For the models with $7D_n$ and $10D_n$ crest widths, the start of damage on the crest occurred at 2.7 and 2.8 stability numbers, respectively, in the total section. Moreover, failure (for $N_0=0.2$) occurred when the stability numbers were 3, 3.15 and 3.8 for the crest widths of $4D_n$, $7D_n$ and $10D_n$, respectively. This means that increasing the crest width delays the damage to the total section. From these evaluations, it was observed that the total section showed a more stable behavior with the increase in the crest width. Keeping in mind that the packing density is low (0.59), these models are not more stable than the single-layer conventional breakwater because, at the intersection between the front slope and crest, the stability of cubes is more affected by the waves for LCBs with single layer regularly placed cube. In the case of a low packing density, stability decreased due to the formation of relatively large gaps between the front slope and the crest due to the separation in the slope after the effect of the waves.

In this study, there was no damage in the front slope of low-crested models for the higher packing density of 0.67, which indicates that the low-crested structures become more stable for higher packing densities. However, even at this higher packing density, damage was observed on the crest for $B=4D_n$ and $7D_n$ but not $10D_n$ since the crest width increases stability. The reasons for the stability increase with increasing crest width are the fact that cube units lean more against each other at wider widths, the distribution of forces due to wave impacts on a wider area, and the increase in the mass of the breakwater. These results are consistent with the literature (Van der Meer, 1988).

For single-layer regular placement in Fig. 7, the relative damage versus the relative freeboard is also plotted for stability in the front slope. As seen in Fig. 7, although the change for regular placement showed a similar trend to irregular placement, less relative damage was determined under the same experimental conditions. In addition, if the relative freeboard is less than 0.6, the increase in damage becomes evident because of increasing wave height and the initial damage occurs later than in irregular placement.

The stability of regularly and irregularly placed models with 0.59 packing density were compared. For the irregularly placed model with

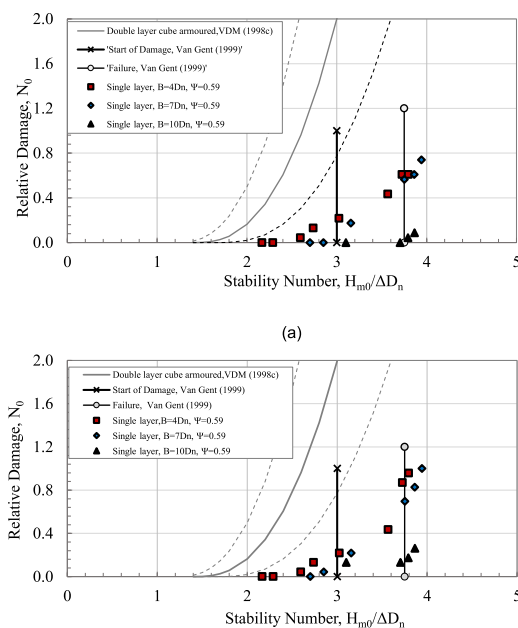


Fig. 12. Relative damage of single-layer cube regular placed breakwater. The dashed lines indicate the boundaries of the 90% confidence interval, (a) Comparative evaluation of relative damage for front slope and (b) Comparative evaluation of relative damage for total section (front slope and crest).

crest widths of $4D_n$, $7D_n$ and $10D_n$, the initial displacements on the front slope were observed as $N_0=2.73$, 2.65 and 2.06, respectively, those are 2.6, 3.2 and 3.8 for regular placed models. The start of damage occurred at 2.59, 2.32 and 1.79 for irregularly placed models however, it occurred at 2.2, 2.9 and 3.7 for regularly placed models with $4D_n$, $7D_n$ and $10D_n$ crest widths, respectively. Single-layer regular placement on the seaward slope is more stable than double-layer irregular placement. However, in single-layer placement, unlike the irregular placement on

the seaward slope, stability increases as the crest width increases. This is due to the cube blocks being placed to lean against each other, the surface being smoother, and increasing resting drag under the wave effect. Similar behavior was observed in crest stability. To ensure a stable cube armoured breakwater with regular placement technique, each unit should contact its several neighboring cubes to increase the friction surface and maximize the resting drag of each other. The intersection from the slope to the crest where the slope changes to

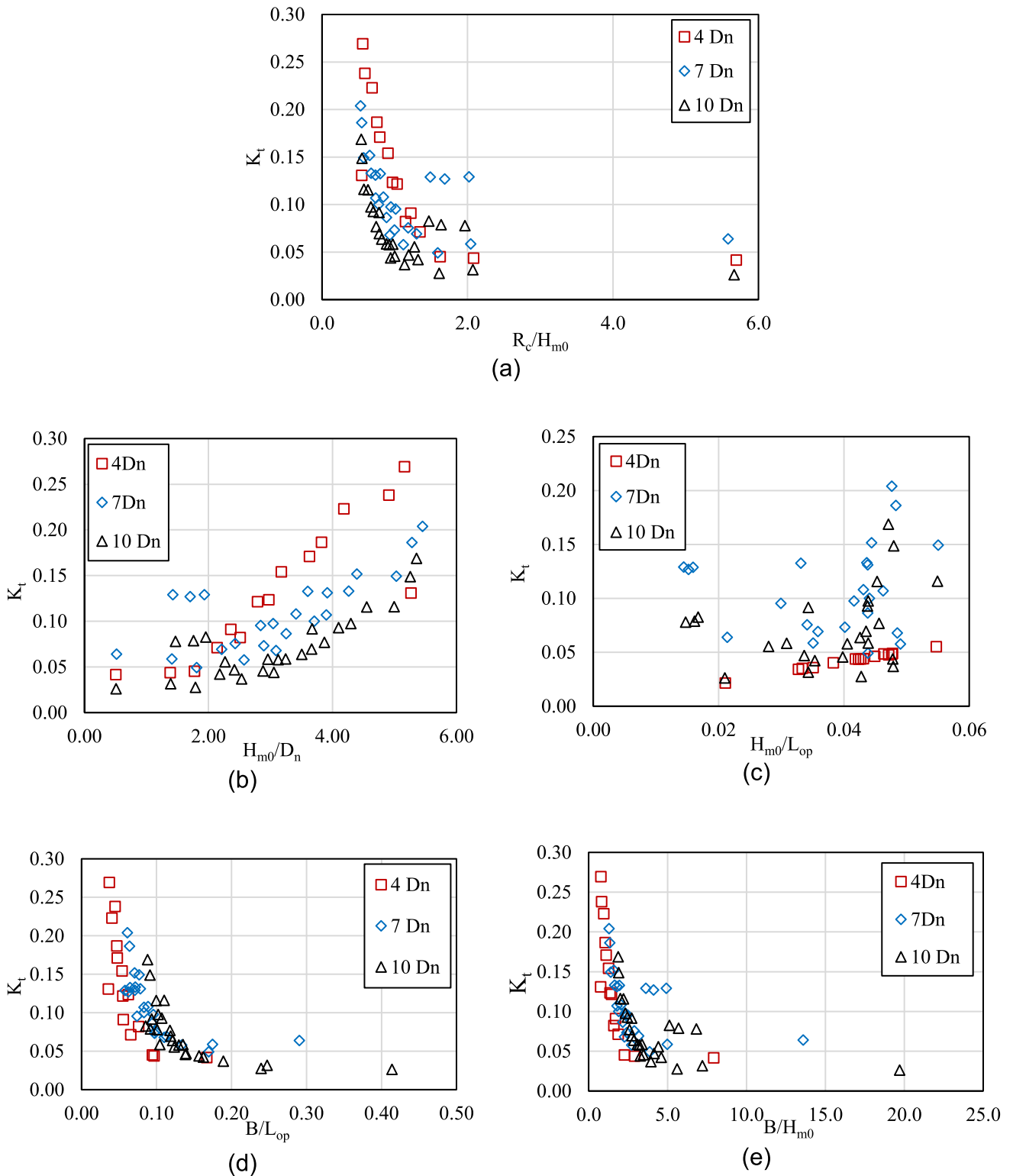


Fig. 13. Transmission coefficient with non-dimensional parameters for irregular double layer placement.

horizontal, causes structural discontinuity hence causing a decrease of contact surface. The edges of the crest are more exposed to wave forces as well. These reasons cause initial damage to start in this region more frequently.

Another issue is the placement of the cubes: It is often difficult to place units at the intersection between crest and slope to achieve the desired crest width. Also, the crest region experiences larger forces and turbulence due to wave breaking and overtopping for LCBs. As soon as initial damage occurs, failure follows. Because of this behavior, Van der Meer (1988) recommended not constructing a low-crested structure with a single-layer cube.

3.2. Hydraulic responses

3.2.1. Wave transmission

Wave transmission is defined as $K_t = H_{m0-t}/H_{m0}$; where H_{m0} is the incident spectral wave height in front of the structure ($H_{m0} = 4\sqrt{m_0}$) and H_{m0-t} is the transmitted spectral wave height behind the structure. Many studies have been conducted on wave transmission for submerged (freeboard $R_c < 0$) and emerged low-crested (freeboard $R_c > 0$) coastal structures. However, this study considered only emerged LCBs with different placements of cubes.

In low-crested structures, wave energy transmission occurs primarily by wave overtopping. Also, wave energy is transmitted through the body of the structure which is more dominant as the crest height increases. For this reason, permeability is primarily important for the breakwaters when overtopping is not allowed or limited. Previous studies stated that wave transmission depends mainly on freeboard (R_c), crest width (B), incident wave height (H_{m0}), wave steepness (s), the slope of the structure ($\tan\alpha$), armour nominal diameter (D_{n50}), porosity (n) and water depth (d). Impermeable structures, on the other hand, show a slightly different performance than permeable structures in terms of wave transmission. d'Angremond et al. (1996) indicated that the same parameters affect wave transmission for impermeable and permeable structures and that the differences can be explained by changing a coefficient in their empirical expression. Their study considered both submerged and emerged structures.

(i) Double Layer Irregular placement

Considering the effective parameters from previous studies on wave transmission in the literature, it has been stated that the seaward slope of LCBs is generally not very effective. In the present study, when a dimensional analysis is performed, the following dimensionless parameters are obtained similar to Kurdistani et al. (2022) and Van der Meer and Daemen (1994). The effects of these dimensionless parameters on wave transmission are examined separately in the following paragraphs.

$$K_t = H_{m0-t}/H_{m0} = f(H_{m0}/D_n, B/H_{m0}, H_{m0}/L_{op}, B/L_{op}, R_c/H_{m0}) \quad (5)$$

The variation of transmission coefficients for three different crest widths of double-layer placement with respect to dimensionless parameters are given in Fig. 13. When these changes are examined, the transmission coefficient increases as the relative wave height increases (H_{m0}/D_n). As seen from the figures, crest width has a significant effect on wave transmission, transmission decreases as the crest width increases. The variation of wave transmission with relative crest width (B/H_{m0}) is quite evident, at $B/H_{m0} < 5$, wave transmission decreases rapidly as the relative crest width increases. The relationship between wave transmission and wave period has been tried to be determined by taking into account the wave steepness, H_{m0}/L_{op} . It is seen that this relationship, considering the peak wave period, does not have a clear trend. Although it is not fully evident, only at wider crest widths, transmission increases with increasing wave period (Figs. 13c and 13d). Additionally, the considered LCB has a single constant slope (1/1.5). For this reason, the influence of the surf-similarity parameter on wave transmission may

also show scatter. However, since the compatibility with the d'Angremond et al. (1996) expression, which includes the surf similarity parameter, was investigated, the surf similarity parameter containing the wave steepness was used in expression 8. While wave steepness versus transmission coefficient for the larger crest widths (the blue and black symbols in Fig. 13c) show a relatively large amount of scatter, narrow crest width (the red symbols) shows a clear relation due to larger wave transmission. The effect of the wave period (or wave length) and crest width was examined with respect to the dimensionless parameter B/L_{op} in Fig. 13d. It can be seen from Fig. 13d that wave transmission increases with increasing wave period (or decreasing wave steepness). This increase is more evident for the narrow crest width. The dimensionless parameter thought to be most effective in wave transmission is the dimensionless crest height (R_c/H_{m0}) in Fig. 13a. As the relative crest height increases, wave transmission decreases significantly. In this way, the effect of crest width is also clearly seen.

The experimental results in this study were compared with the studies given in the literature on both emerged and submerged breakwaters. Eight studies (d'Angremond et al., 1996; Van der Meer, 1990; Daemen, 1991; Muttray et al., 2006; Goda and Ahrens, 2008; Tomasicchio and D'Alessandro, 2013; Giantsi and Moutzouris, 2016; Van Gent et al., 2023) were considered in the literature. In these studies, the quarry stone was taken into consideration in general for the armour layer, and some of these studies were on submerged and some of them were on emerged breakwaters, or transmission coefficients were found by taking both submerged and emerged case combinations into consideration.

In this study, RMSE (root mean square error) and R^2 (determination coefficient) values were calculated by considering these studies separately (Table 5) as follows:

$$RMSE = \sqrt{\frac{1}{N} \sum_{i=1}^N (C_i - M_i)^2} \quad (6)$$

$$R = \frac{\sum_{i=1}^N [(C_i - \bar{C})(M_i - \bar{M})]}{\sqrt{\sum_{i=1}^N (C_i - \bar{C})^2 \sum_{i=1}^N (M_i - \bar{M})^2}} \quad (7)$$

where N is the sample size, M_i is the measured value, C_i is the calculated value, \bar{M} and \bar{C} are sample mean of the measured and calculated values, respectively, and R is the correlation coefficient.

In this study, the expression given by d'Angremond et al. (1996) gives the best fit as the experimental conditions are close to the present study. Despite this good match, the expression given by d'Angremond et al. (1996) predicts higher transmission (Fig. 14). The reason for the differences between some of the expressions in literature and the data from this study is due to the fact that wave reflections are not analyzed sufficiently, and regular wave conditions are taken into account, especially in older studies. Moreover, cube armoured structures were used in this study.

The wave transmission coefficient equation obtained in this study is from a revised form of d'Angremond et al. (1996)'s expression. The new best-fitted expression (8) is obtained as follows.

$$K_{t1} = -0.21 \frac{R_c}{H_{m0}} + 0.39 \left(\frac{B}{H_{m0}} \right)^{-0.28} (1 - e^{-0.5\zeta}) \quad (8)$$

The boundary conditions of the expression are

$$3.4 < \zeta_{op} < 7, \quad 0.04 < B/L_{op} < 0.4, \quad 0.5 < R_c/H_{m0} < 2.1$$

The relationship between calculated K_t from d'Angremond et al. (1996)'s equation with measured K_t is shown in Fig. 14. The transmission coefficient (K_t) measured in this study versus the revised new fitted one is shown in Fig. 15.

The other most recent equation, given by Van Gent et al. (2023), has also been adapted to the measurements in this study. Since this

Table 5
Statistical values of previous studies and this study.

Authors	Regular						Irregular	
	$\psi=0.59$ and $\psi=0.67$		$\psi=0.59$		$\psi=0.67$		$\psi=0.59$	
	RMSE	R ²	RMSE	R ²	RMSE	R ²	RMSE	R ²
Van der Meer (1990)	0.10	0.52	0.11	0.49	0.10	0.56	0.10	0.49
Daemen (1991)	0.50	0.45	0.50	0.41	0.50	0.48	0.51	0.61
Van der Meer and Daemen (1994)	0.11	0.36	0.11	0.35	0.11	0.38	0.12	0.53
d'Angremond (1996)	0.06	0.92	0.06	0.91	0.06	0.95	0.05	0.76
Muttray et al. (2006)	0.18	0.30	0.18	0.28	0.18	0.32	0.11	0.40
Goda and Ahrens (2008)	0.30	0.02	0.29	0.02	0.31	0.02	0.24	0.12
Tomasicchio and D'Alessandro (2013)	0.29	0.38	0.28	0.47	0.30	0.33	0.06	0.51
Giantsi and Moutzouris (2016)	0.39	0.50	0.39	0.49	0.39	0.52	0.23	0.46
Van Gent et al. (2023)	0.06	0.73	0.06	0.70	0.06	0.76	0.10	0.49
Present Study (Revised from d'Angremond, 1996 Formula)	0.03	0.92					0.02	0.82
Present Study (Revised from Van Gent et al, 2023 Formula)	0.02	0.94					0.02	0.85

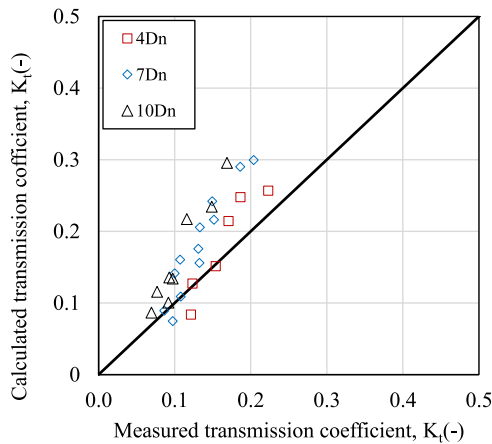


Fig. 14. Transmission coefficients (K_t) measured in this study versus calculated using the expression given by d'Angremond et al. (1996).

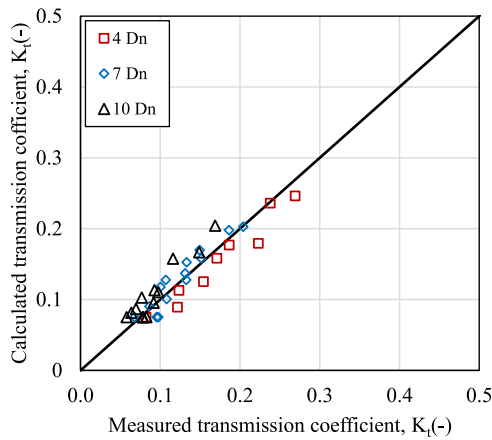


Fig. 15. Transmission coefficient (K_t) measured in this study versus calculated using the revised d'Angremond et al. (1996) expression.

expression takes into account the effects of both the crest freeboard and the crest width, it was adapted and reformulated for the emerged LCBs with a cube armoured layer.

$$K_{t2} = 0.495 \tanh \left(-1.2 \left(\frac{R_c}{H_{m0}} + 4.5 \left(\frac{B}{L_{m-1.0}} \right)^{0.566} - 0.50 \right) \right) + 0.523 \quad (9)$$

(ii) Single Layer Regular Placement

Wave transmission measurements in single-layer models with regular placement with two different packing densities (0.59 and 0.67) were carried out under the same wave conditions as in the double-layer case. Wave transmission analysis was found to have similar trends as the double-layer irregular placement case as shown in Fig. 16. For this case, the effect of packing density on wave transmission was also investigated.

Fig. 16a shows the effects of packing density, crest width and relative freeboard on the transmission coefficient. It can be seen from the figure that the transmission coefficient decreases as the relative freeboard increases for all crest widths. Moreover, as the crest width increases, the transmission coefficient decreases as expected.

In the model with $B=4D_n$ crest width, it was observed that the lower packing density of 0.59 caused a slightly larger transmission than the packing density of 0.67. This is thought to be due to the contribution of transmission due to penetration through structure at lower packing density. For $B=7D_n$ crest width, no effect of the packing density on the transmission performance was observed, all data almost overlapped in two different packing densities. It is observed that in the model with $B=10D_n$ crest width, the effect of the packing density of the cube blocks on the transmission is measured to be slightly greater for $\psi=0.67$, than $\psi=0.59$. This result is the opposite of the observation determined for $4D_n$ width. In this case, as the crest width increases, the wave transmission with penetration becomes less and transmission is dominated by wave overtopping that is, the wave overtopping is more dominant than the wave penetration since larger packing density causes smooth surface and more run up hence wave overtopping.

Considering two different packing densities of single-layer placement, wave transmission was compared with previous studies as done in double-layer placement. d'Angremond et al. (1996) expression was compared with measurement data, this expression provides the best fit with the data among the previous studies, yet it overestimates transmission coefficients. Van Gent et al. (2023) is the most up-to-date study in the literature. The calculated transmission coefficients using this expression agreed well with the measured values. As a result, when comparing the studies of all researchers with measurements, as the crest width increases, the agreement between the measurement and calculated transmission coefficients gradually decreases.

The expression given by d'Angremond et al. (1996) was re-fitted and compared with the transmission coefficients measured from single-layer cube models with three different crest widths and two different packing densities in the armour layer. The new expression is found as given in Eq. (10). Similarly, the second-best expression is given in Eq. (11), obtained by refitting the Van Gent et al. (2023) formula. Since the effect of packing density is minor, it is not considered in equations. The variation of measured and predicted transmission coefficients by re-evaluation of d'Angremond et al. (1996) and Van Gent et al. (2023) formulas are presented in Fig. 17a and b, respectively.

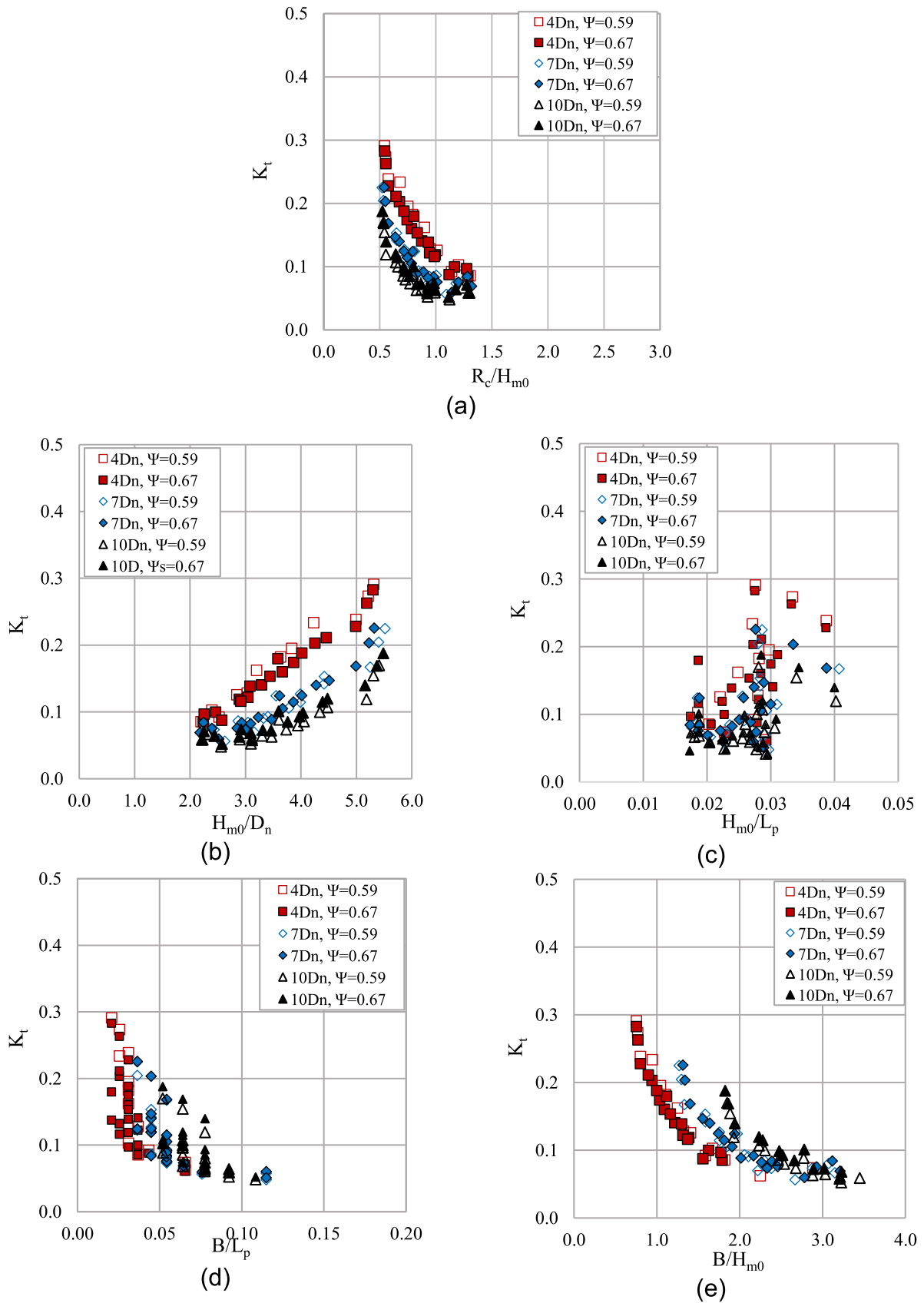
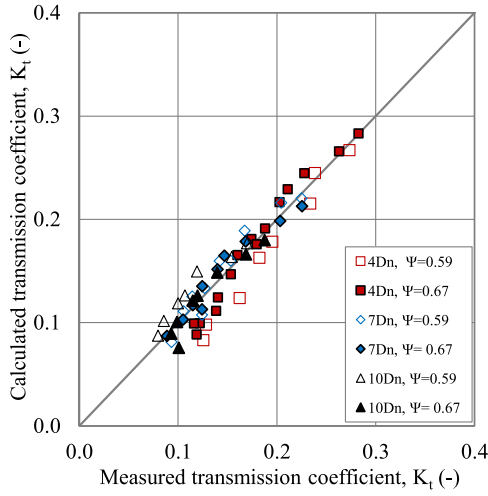
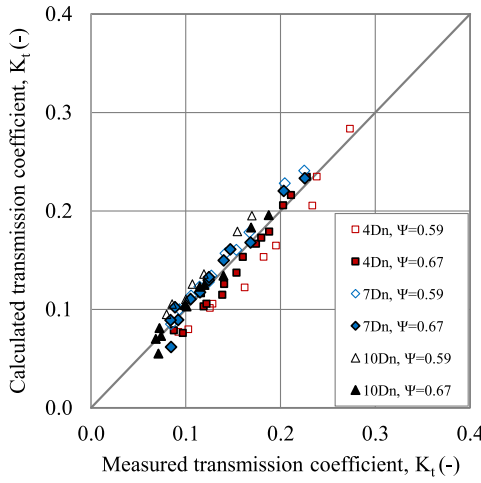


Fig. 16. Transmission coefficient versus non-dimensional parameters for regular single-layer placement.



(a)



(b)

Fig. 17. Transmission coefficients (K_t), (a) Transmission coefficient (K_t) in this study versus revised d'Angremond et al. (1996) for regular placement and (b) Transmission coefficient (K_t) in this study versus revised Van Gent et al. (2023) for regular placement.

$$K_{t1} = -0.279 \frac{R_c}{H_{m0}} + \left(0.4403 \times \left(\frac{B}{H_{m0}} \right)^{-0.32} \times \left(1 - e^{(-0.576\xi_p)} \right) \right) \quad (10)$$

$$K_{t2} = 0.47 \tanh \left(-1.198 \left(\frac{R_c}{H_{m0}} + 4.678 \left(\frac{B}{L_{m-1.0}} \right)^{0.578} - 0.54 \right) \right) + 0.514 \quad (11)$$

The boundary conditions of the expression are

$$3.3 < \xi_{op} < 5, \quad 0.015 < B/L_{op} < 0.09, \quad 0.5 < R_c/H_{m0} < 1.3$$

Formulas of the wave transmission coefficient include only wave height information. However, the wave spectrum provides information about wave height, wave period and energy distribution. The spectrum densities obtained from measurements at the toe of the model, and the spectrum densities of the incident and transmitted waves are given in Fig. 18. It can be seen from this figure that the energy of the transmitted wave has decreased significantly.

Normalized incident and transmitted wave energy density spectra are given together in Fig. 19, since the spectrum of the transmitted wave is much smaller than the incoming wave spectrum, non-dimensional spectra were used so that they can be evaluated together. For LCBs, both the wave propagation over the structure and through the structure contribute to energy transfer to the rear side of the structure. The spectral shape of the transmitted wave is very similar to that of the incoming spectrum up to $1.5f_p$. For higher frequencies, the spectral shape changes, where f_p is the peak wave frequency. In the $1.5 < f/f_p < 3.5$ part, the spectrum has a secondary peak at the double frequency of the peak frequency similar to that observed by Van Gent et al. (2023). Observations show that the transmitted wave periods at the back of the model decrease. The energy level decreases with increasing frequency of the wave energy spectrum (decreasing period, $T_{m-1.0}$). As expected, observations showed that, as the crest width increases, the energy of the transmitted wave decreases, but the spectra show a similar shape, while the second crest decreases and becomes flatter.

3.2.2. Wave reflection

With the experimental conditions considered in this study, wave reflection by low-crested stable (emerged) breakwaters was also examined. Since the observations showed that the wave reflection coefficient results were very close to each other for both single and double-layer placements, both situations were evaluated together. First, the change of reflection coefficient ($K_r = H_{m0r}/H_{m0i}$) versus wave steepness, where the spectral period is considered, is shown in Fig. 20. As can be seen from this figure, the wave reflection coefficient shows a linear decrease as the wave steepness increases.

The variation of the reflection coefficient with the relative freeboard is shown in Fig. 21. The reflection coefficient decreases as the relative freeboard increases up to 1.25 and continues to increase after this relative freeboard.

A significant effect of the relative crest width on the reflection coefficient is observed for both regular and irregular placements (Fig. 22). This figure also shows the effect of the wave period such that reflection increases for waves with longer wave periods.

Zanutigh and Van der Meer (2008) considered emerged narrow and LCBs in the derivation of the reflection equation in their study. The researchers stated that the reflection decreases in LCBs hence they adjusted the expression given for conventional breakwaters by only adding a relative freeboard effect. However, in this study, the effect of relative crest width was also considered, and the expression given by Zanutigh and Van der Meer (2008) was reformulated as follows. The error (RMSE) in this new expression was found to be 0.06.

$$K_r = \left(\tanh \left(a \cdot \frac{B}{\xi_0} \right) \right) \cdot \left(0.96 + 0.37 \frac{R_c}{H_{m0}} \frac{B}{L_{m-1.0}} \right) \quad (12)$$

$$a = 0.167 \cdot \left[1 - \exp \left(-3.2 \cdot \gamma_f \right) \right], \quad b = 1.49 \cdot \left(\gamma_f - 0.38 \right)^2 + 0.86$$

where the friction factor (γ_f) is 0.47 for double-layer placement and 0.5 for single-layer placement of cubes. The validity limits of this formula are as follows.

$$3.10 \leq \xi_{m-1.0} \leq 6.53, \quad 0.45 \leq \frac{R_c}{H_{m0}} \leq 2.1, \quad 0.015 \leq \frac{B}{L_{m-1.0}} \leq 0.184.$$

Eq. 10 is valid in the limited conditions of the presented experiments. That is why, as also indicated by Zanutigh and Van der Meer (2008), more data are needed to allow a proper check and improvement of Eq. 10. In the present study, experimental results showed that the average reflection coefficients were 0.42 and 0.45 for single and double layer placements, respectively.

Wave energy is damped due to the interaction of the wave with the structure. Factors effective in dissipating energy are explained as wave transmission, wave reflection and roughness. The energy dissipation due

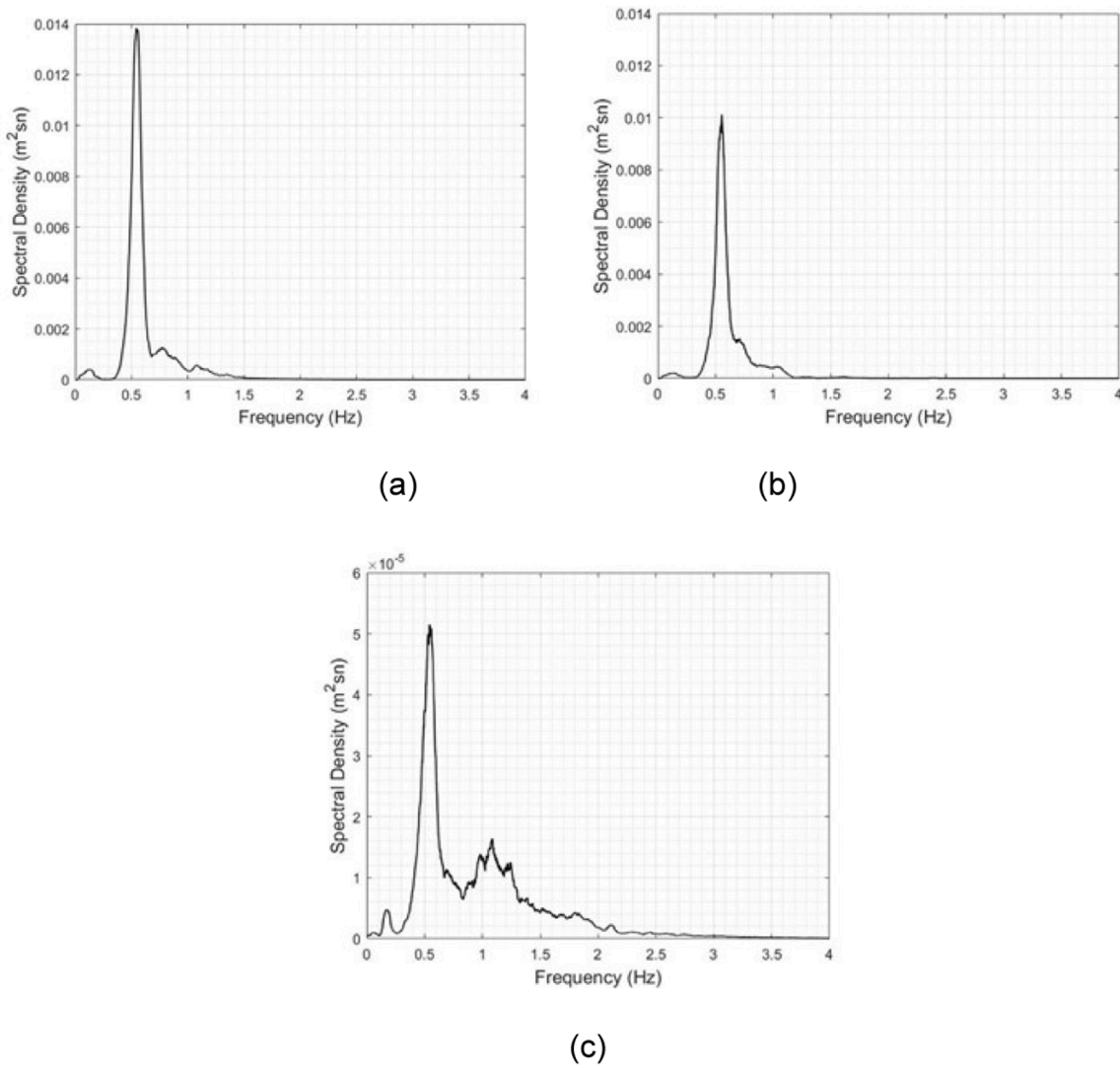


Fig. 18. Wave spectra for $B=4D_n$ and “ $H_{m0}=0.15m$ and $T_p=1.8s$ ”, (a) Measured wave, (b) Incident wave and (c) Transmitted wave.

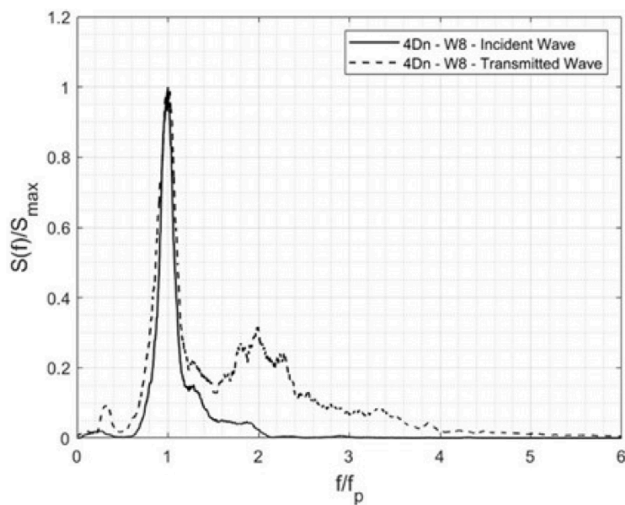


Fig. 19. Incident and transmitted dimensionless wave spectra for $B=4D_n$ and “ $H_{m0}=0.15m$ and $T_p=1.8s$ ”.

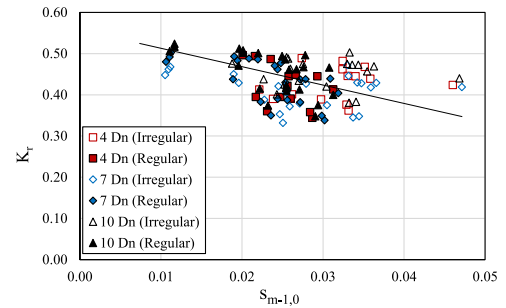


Fig. 20. Reflection coefficient versus wave steepness.

to wave transmission and wave reflection is calculated by Eq. (13). Fig. 23 shows the change in energy dissipation with relative freeboard in the range of $0.5 < R_c/H_{m0} < 2.1$. The remaining energy from reflection and wave transmission is dissipated by armour layer roughness which depends on placement type, wave refraction and permeability of the structure. The energy dissipation increases for relative freeboards between 0.5 and 1.0, because at small values of the relative freeboard around 0.5, it is exposed to waves larger than the design wave and the wave overtopping is larger, thus the wave energy is transmitted to the rear side of the LCB. On the other hand, when the relative freeboard

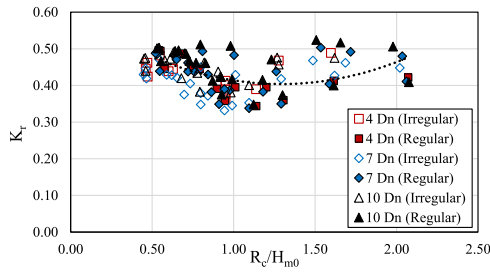


Fig. 21. Reflection coefficient versus relative crest freeboard.

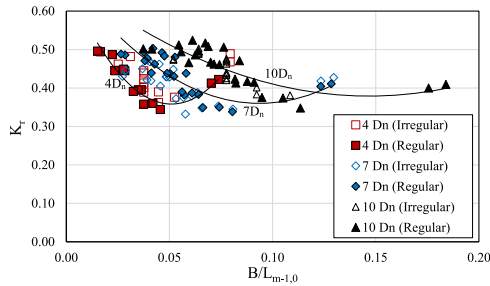


Fig. 22. Reflection coefficient against relative crest width.

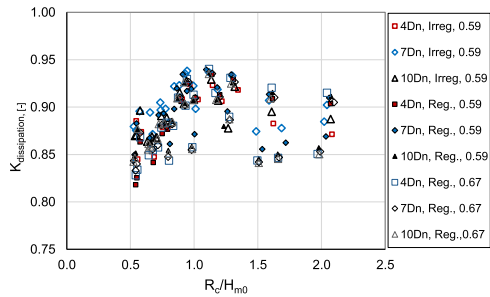


Fig. 23. Energy dissipation against relative crest width.

reaches the value of 1, a highly turbulent flow structure occurs at the front slope due to wave reflection and run-up, and hence energy dissipation increases. However, for relative freeboard values between 1.0 and 1.5, a slight decrease in energy dissipation occurs with the decrease in wave height. The amount of wave dissipation remains constant after the relative freeboard is 1.5 because above this value smaller waves interact with the structure and wave transmission decreases.

$$K_{dissipation} = \sqrt{(1 - K_t^2 - K_r^2)} \quad (13)$$

4. Conclusion

In this study, statically stable emerged LCBs with cube armour layers were investigated experimentally using different placement techniques. This study was carried out under the following boundary conditions:

$$0.018 < s_{m-1,0} < 0.032, \quad 0.04 < B/L_{op} < 0.4 \quad \text{and} \quad 0.45 < R_c/H_{m0} < 2.1.$$

Cubes were used in a double-layer with irregular placement and a packing density of 0.59 and in a single-layer with regular placement and packing densities of 0.59 and 0.67. The main conclusions are listed below.

Structural stability:

1- For structures with a double-layer irregular placement, a similar progression of damage was observed for all crest widths. Although the initial damage started slightly earlier at structures with a larger crest

width ($10D_n$), damage progression is generally very similar for all crest widths. The damage at the front slope of the LCB is smaller compared to the conventional breakwater due to wave overtopping which transfers wave energy to the rear slope. The stability expression given for conventional breakwaters with limited wave overtopping can also be used for the stability of LCBs with a double layer of irregularly placed cubes by reducing the nominal diameter of cubes using a reduction expression. Within the ranges of the test conditions of this research, the diameter of cubes in LCBs can be reduced by approximately 25% compared to the cubes in conventional breakwaters with limited wave overtopping. This corresponds to a reduction in weight of more than a factor of two. The experiments with cubes in a double-layer placement showed that the relative damage (N_0) decreases as the relative freeboard increases (R_c/H_{m0}). However, the damage increases for cases with a relative freeboard of less than 0.6. It was also found that the damage progression does not significantly change with the crest width.

Movements and displacements of double-layer cubes begin primarily in the first row of cubes at the crest. As the wave height increased, the mobility of cubes in the other rows of the crest increased. The mobility of cubes in the rear slope was observed only as M1-type movement that is a displacement of less than $0.5D_n$. There were no $1.0D_n$ displacements in the rear slope for cubes in a double-layer placement.

2- For breakwaters with single-layer cubes, damage did not occur on the seaward slope for the high packing density case ($\psi=0.67$). Although the stability of a single-layer cube armoured LCB is larger than the stability of a double-layer breakwater with the same packing density ($\psi=0.59$), crest damage on the single-layer cube breakwater causes instability of the cubes. The structural stability of LCBs with single-layer cubes showed different responses compared to the double-layer case due to the regular placement and also the geometric discontinuity at the transition between the seaward slope and the crest. The position of this discontinuity is exposed to large wave forces leading to a relatively weak spot in the armour layer. There was no damage in the rear slope for both packing densities of the single layers.

Hydraulic response:

3- The crest width of cube armoured LCBs has a significant effect on wave transmission, and as the crest width increases, transmission decreases. The decrease in wave transmission with relative crest width (B/H_{m0}) is quite evident for relative crest widths smaller than 5 ($B/H_{m0} < 5$). Wave transmission increases with increasing period which is more prominent for narrow crest widths. When the relative freeboard increases, wave transmission decreases significantly. Within the limits of this study, no effect of wave steepness on wave transmission was observed. It has been found that the expression given by Van Gent et al (2023) can be used with new coefficients for wave transmission at LCBs with cube armor layers, both for irregular two-layer and single-layer placements.

The experiments have shown that at LCBs, the shape of the energy density spectrum of the transmitted wave is similar to that of the incoming spectrum up to $1.5f_p$. For higher frequencies, in the $1.5 < f_p < 3.5$ part, a secondary peak occurs around the double frequency of the peak frequency.

4- Within the limitations of this study, wave reflection at cube armoured LCBs was somewhat lower than for conventional breakwaters. A clear effect of the crest width and the crest freeboard on wave reflection was observed. Also, the reflection coefficient was slightly lower for irregularly placed cubes in a double layer than for regularly placed cubes in a single layer. The expression given by Zanuttigh and Van der Meer (2008) can be used with new coefficients for wave reflection in LCBs with cube armor layers, both in irregular two-layer and single-layer placements.

Future work:

In future studies, the structural and hydraulic behaviors of submerged and crest is at water level breakwaters with concrete blocks can be investigated experimentally. Furthermore, the hydraulic behavior of low-crest breakwaters can be modeled using numerical methods.

CRediT authorship contribution statement

Yalcin Yuksel: Writing – original draft, Supervision, Methodology, Investigation, Conceptualization. **Esin Cevik:** Writing – review & editing, Visualization, Investigation, Conceptualization. **Cihan Sahin:** Writing – review & editing, Investigation, Conceptualization. **Marcel R. A. van Gent:** Writing – review & editing, Methodology, Conceptualization. **Serhat Gumus:** Visualization, Investigation, Data curation. **Duygu Issever:** Visualization, Investigation, Data curation. **Umutcan Inal:** Visualization, Investigation, Data curation. **Mehmet Utku Ogur:** Visualization, Investigation, Data curation.

Declaration of competing interest

The authors declare that they have no known competing financial interests or personal relationships that could have appeared to influence the work reported in this paper.

Acknowledgement

This research is supported by the Research Fund of the Yildiz Technical University, project number: FCD-2024–6394. The authors are also grateful to FIBROBETON.

References

- Ahrens, J.P., 1987. Characteristics of Reef Breakwaters. US Army Corps of Engineers. Technical Report CERC, 87-17.
- Ahrens, J.P., 1989. Stability of reef breakwaters. *J. Waterway, Port, Coastal Ocean Eng.*, ASCE 115 (2), 221–234.
- Andersen, T.L., Burcharth, H.F., 2010. A new formula for front slope recession of berm breakwaters. *Coastal Eng.* 57 (4), 359–374. <https://doi.org/10.1016/j.coastaleng.2009.10.017>.
- Briganti, R., Van der Meer, J., Buccino, M., Calabrese, M., 2003. Wave transmission behind low-crested structures. In: International Conference on Coastal Structures 2003. Portland, Oregon, USA, pp. 580–592. [https://doi.org/10.1061/40733\(147\)48](https://doi.org/10.1061/40733(147)48).
- Buccino, M., Calabrese, M., 2007. Conceptual approach for prediction of wave transmission at low-crested breakwaters. *J. Waterway, Port, Coastal, Ocean Eng.*, ASCE 133 (3), 213–224. [https://doi.org/10.1061/\(ASCE\)0733-950X\(2007\)133:3\(213\)](https://doi.org/10.1061/(ASCE)0733-950X(2007)133:3(213)).
- Burcharth, H.F., Kramer, M., Lamberti, A., Zanuttigh, B., 2006. Structural stability of detached low crested breakwaters. *Coastal Eng.* 53 (4), 381–394. <https://doi.org/10.1016/j.coastaleng.2005.10.023>.
- Burger, G., 1995. Stability of Breakwaters With Low Crest (in Dutch). TU Delft. Master thesis.
- Calabrese, M., Vicinanza, D., Buccino, M., 2002. Large-scale experiments on the behaviour of low crested and submerged breakwaters in presence of broken waves. In: 28 th. International Conference on Coastal Engineering (ICCE) 2002. Cardiff, Wales. World Scientific, pp. 1900–1912. https://doi.org/10.1142/9789812791306_0160.
- Daemen, I.F.R., 1991. Wave Transmission at Low Crested Structures. TU Delft. Master thesis. <http://resolver.tudelft.nl/uuid:433dfcf3-eb87-4dc9-88dc-8969996a6e3f>.
- d'Angremond, K., Van der Meer, J.W., De Jong, R.J., 1996. Wave transmission at low-crested structures. In: 25 th. International Conference on Coastal Engineering (ICCE) 1996. Orlando, Florida, pp. 2418–2427. <https://doi.org/10.1061/9780784402429.187>.
- Frens, A.B., 2007. The Impact of Placement Method On Antifer-block stability. TU Delft. <https://doi.org/10.4233/uuid:0528aadB-3415-43d0-876e-b0f399395030>. Master thesis.
- Guo, Y.C., Mohapatra, S.C., Guedes Soares, C., 2022. Experimental study on the performance of an array of vertical flexible porous membrane type breakwater under regular waves. *Ocean Eng.* 264, 112328. <https://doi.org/10.1016/j.oceaneng.2022.112328>.
- Guo, Y.C., Mohapatra, S.C., Guedes Soares, C., 2023a. An experimental study on the performance of combined membrane breakwaters against incident waves. *Ocean Eng.* 280, 114793. <https://doi.org/10.1016/j.oceaneng.2023.114793>.
- Guo, Y.C., Mohapatra, S.C., Guedes Soares, C., 2023b. Experimental performance of multi-layered membrane breakwaters. *Ocean Eng.* 280, 114793. <https://doi.org/10.1016/j.oceaneng.2023.114716>.
- Giantsi, T., Moutzouris, C.I., 2016. Experimental investigation of wave transmission and reflection at a system of low crested breakwaters. In: 13th International Conference on Protection and Restoration of the Environment. <https://doi.org/10.1007/s40710-017-0237-8>.
- Givler, D.L., Sorensen, R.M., 1986. An Investigation of the Stability of Submerged Homogeneous Rubble-Mound Structures Under Wave Attack. H. R. Imb Hydrolics Laboratory, Department of Civil Engineering, Lehigh University, Bethlehem, PA. Report No. HL-110-86.
- Goda, Y., Ahrens, J.P., 2008. New formulation of wave transmission over and through low-crested structures. In: 31 th. International Conference on Coastal Engineering (ICCE) 2008. Hamburg, Germany, 5. World Scientific, pp. 3530–3541. <https://doi.org/10.1142/7342>.
- Hughes, S.A., 1993. Physical Models and Laboratory Techniques in Coastal Engineering, 7. World Scientific. <https://doi.org/10.1142/2154>.
- Kurdistani, S.M., Tomasicchio, G.R., Felice, D., Francone, A., 2022. Formula for wave transmission at submerged homogeneous porous breakwaters. *Ocean Eng.* 266, 113053. <https://doi.org/10.1016/j.oceaneng.2022.113053>.
- Mansard, E.P., Funke, E.R., 1980. The measurement of incident and reflected spectra using a least squares method. In: 17 th. International Conference on Coastal Engineering (ICCE) 1980. Sydney, Australia, pp. 154–172. <https://doi.org/10.1061/9780872622647.008>.
- Muttray, M., Oumeraci, H., Ten Oever, E., 2006. Wave reflection and wave run-up at rubble mound breakwaters. 30 th. In: International Conference on Coastal Engineering (ICCE) 2006. San Diego, California, USA, 5. World Scientific, pp. 4314–4324. https://doi.org/10.1142/9789812709554_0362.
- Muttray, M., Ten Oever, E., Reedijk, B., 2012. Stability of low crested and submerged breakwaters with single layer armouring. *J. Shipping Ocean Eng.* 2, 140–152.
- Powell, K.A., Allsop, W., 1985. Low-crest breakwaters, Hydraulic Performance and Stability. HR Wallingford. Report SR 57. <https://eprints.hrwallingford.com/97/>.
- Rock Manual. (2007). The use of rock in hydraulic engineering (2nd ed.). C683. CURIA, CUR, CETMEF: London.
- Seabrook, S.R., & Hall, K.R. (1998). Wave transmission at submerged rubblemound breakwaters. <https://doi.org/10.1061/9780784404119.150>.
- Sindhu, S., Shiral, K.G., 2015. Prediction of wave transmission characteristics at submerged reef breakwater. *Procedia Eng.* 116, 262–268. <https://doi.org/10.1016/j.proeng.2015.08.289>.
- Tomasicchio, G.R., & D'Alessandro, F. (2013). Wave energy transmission through and over low crested breakwaters. *J. Coastal Res.*, 65, 398–403. <https://doi.org/10.2112/SI65-068.1>.
- Van der Meer, J.W. & Pilarczyk, K.W. (1990). Stability of low-crested and reef breakwaters. Delft Hydraulics report no. H986, prepared for CUR C67. <https://doi.org/10.1061/97808726227765.105>.
- Van der Meer, J.W., 1988. Deterministic and probabilistic design of breakwater armor layers. *J. Waterway, Port, Coastal, Ocean Eng.* 114 (1), 66–80. [https://doi.org/10.1061/\(ASCE\)0733-950X\(1988\)114:1\(66\)](https://doi.org/10.1061/(ASCE)0733-950X(1988)114:1(66)). ASCE.
- Van der Meer, J.W., 1990. Data On Wave Transmission Due to Overtopping. Delft Hydraulics. <https://books.google.com.tr/books?id=Xni-tgAACAAJ>.
- Van der Meer, J.W. (1990a). Low-crested and reef breakwaters. Delft Hydraulics Report H 198/Q 638.
- Van der Meer, J.W., 1999. Design of concrete armour layers. In: *Proceedings of the coastal structures 99. Spain*, pp. 213–221.
- Van der Meer, J.W., Daemen, I.F., 1994. Stability and wave transmission at low-crested rubble-mound structures. *J. Waterway, Port, Coastal Ocean Eng.* 120 (1), 1–19. [https://doi.org/10.1061/\(ASCE\)0733-950X\(1994\)120:1\(1\)](https://doi.org/10.1061/(ASCE)0733-950X(1994)120:1(1)). ASCE.
- Van der Meer, J.W., Briganti, R., Zanuttigh, B., Wang, B., 2005. Wave transmission and reflection at low-crested structures: design formulae, oblique wave attack and spectral change. *Coastal Eng.* 52 (10–11), 915–929. <https://doi.org/10.1016/j.coastaleng.2005.09.005>.
- Van Gent, M.R.A., 2003. Recent developments in the conceptual design of rubble mound breakwaters. In: COPEDEC VI. Colombo, Sri Lanka.
- Van Gent, M.R.A., 2013. Rock stability of rubble mound breakwaters with a berm. *Coastal Eng.* 78, 35–45. <https://doi.org/10.1016/j.coastaleng.2013.03.003>.
- Van Gent, M.R.A., Buis, L., Van den Bos, J.P., Wüthrich, D., 2023. Wave transmission at submerged coastal structures and artificial reefs. *Coastal Eng.* 184. <https://doi.org/10.1016/j.coastaleng.2023.104344>.
- Van Gent, M.R.A., Plate, S.E., Berendsen, E., Spaan, G.B.H., Van der Meer, J.W., d'Angremond, K., 1999. Single-layer rubble mound breakwaters. In: *Proc. Coastal Structures 99. Santander, Spain*. ASCE.
- Vidal, C., Losada, M.A., Mansard, E.P., 1995. Stability of low-crested rubble-mound breaker heads. *J. Waterway, Port, Coastal Ocean Eng.*, ASCE 121 (2), 114–122.
- Vidal, C., Losada, M.A., Medina, R., Mansard, E.P.D., Gomez-Pina, G., 1992. A universal analysis for the stability of both low-crested and submerged breakwaters. In: 23 rd. *International Conference on Coastal Engineering (ICCE) 1992*. Venice, Italy, pp. 1679–1692. <https://doi.org/10.1061/9780872629332.127>.
- Wolters, G., Van Gent, M., Allsop, W., Hamm, L., Muhlestein, D., 2010. HYDRALAB III: guidelines for physical model testing of rubble mound breakwaters. In: *Coasts, marine structures and breakwaters: Adapting to change: Proceedings of the 9th international conference organised by the Institution of Civil Engineers and held in Edinburgh on 16 to 18 September 2009*. Thomas Telford Ltd, pp. 559–670. <https://doi.org/10.1680/cmsb.41318.0062>.
- Yuksel, Y., Cevik, E., Van Gent, M.R.A., Sahin, C., Altunsoy, A., Yuksel, Z.T., 2020. Stability of berm type breakwater with cube blocks in the lower slope and berm. *Ocean Eng.* 217, 107985. <https://doi.org/10.1016/j.oceaneng.2020.107985>.
- Yuksel, Y., Van Gent, M.R.A., Cevik, E., Kaya, A.H., Ari Guner, H.A., Yuksel, Z.T., Gumuscu, I., 2022. Stability of high density cube armoured breakwaters. *Ocean Eng.* 253. <https://doi.org/10.1016/j.oceaneng.2022.111317>.
- Zanuttigh, B., Van der Meer, J.W., 2008. Wave reflection from coastal structures in design conditions. *Coastal Eng.* 55, 771–779. <https://doi.org/10.1016/j.coastaleng.2008.02.009>.
- Zhang, S., Li, X., 2014. Design formulas of transmission coefficients for permeable breakwaters. *Water Sci. Eng.* 7 (4), 457–467, 10.3882.